Alpine snowpit profiles of polar organic compounds from Mt. Tateyama central Japan: Atmospheric transport of organic pollutants with Asian dust

Ambarish Pokhrel[1,4,5], Kimitaka Kawamura[1,2*] Eri Tachibana[1], Bhagawati Kunwar[1,2], and Kazuma Aoki[3]

[1]Institute of Low Temperature Science, Hokkaido University, Sapporo, Japan

[2]Chubu Institute for Advanced Studies, Chubu University, Kasugai, Japan

[3]Department of Earth Science, Faculty of Science, Toyama University, Toyama, Japan

[4]Institute of Science and Technology (IOST), Tribhuvan University, Nepal

[5]Asian Research Center, Kathmandu, Nepal

[*]Corresponding author (K. Kawamura: kkawamura@isc.chubu.ac.jp)

Revised to Atmospheric Environment

Keywords

Diacids, Incloud isoprene oxidation, snowpit, Asian dust, Transboundary pollutions

Highlights

1. Bacteria and Incloud isoprene oxidation results in the end product of dicarboxylic acids.
2. Organic compounds are attributed to heterogeneous reactions.
3. Atmospheric transport of diacids and oxoacids with Asian dust is important.
4. Asian dust is not responsible for the atmospheric photochemical processing of organics.
5. Snow metamorphism may play an important role in these organic compounds (fresh organic compounds are well captured).

Graphical Abstract

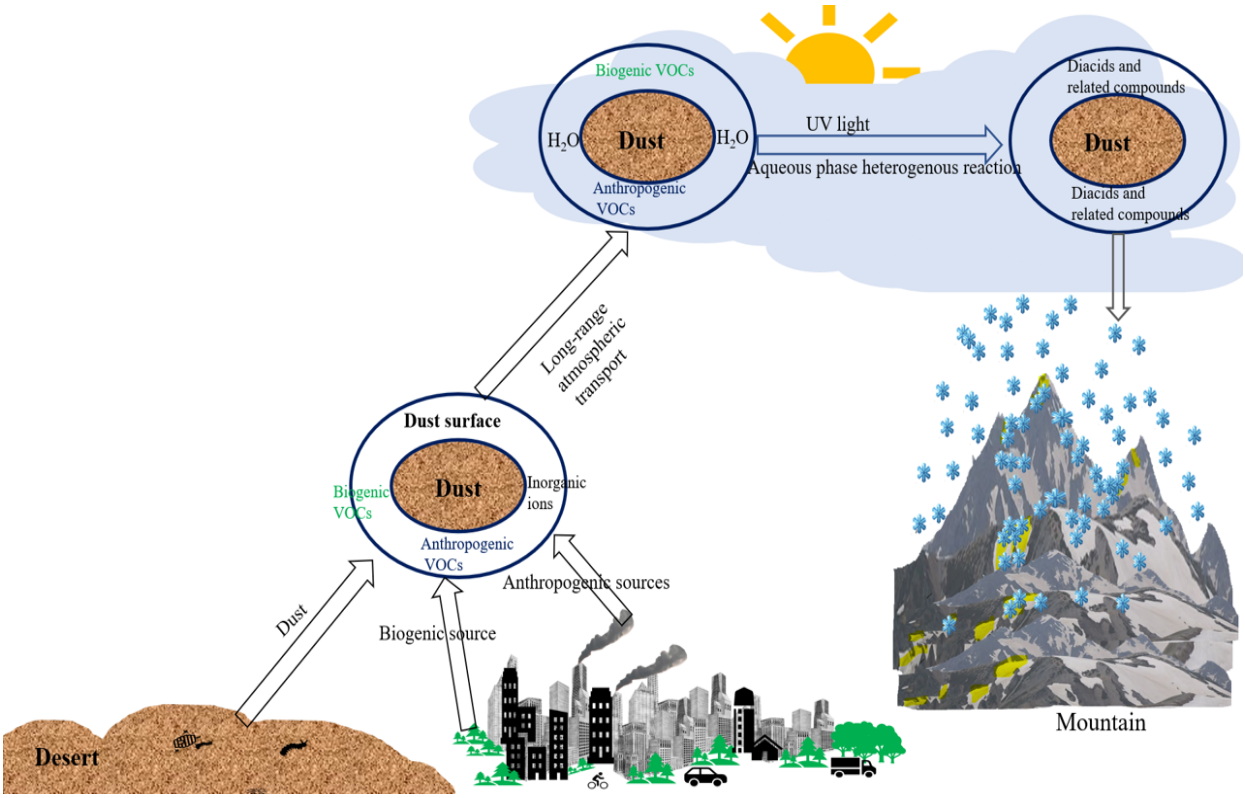

Abstract

Snowpit samples (n =10) were collected (19 April 2008) from the snowpit sequences (depth 6.60 m) at the Murodo-Daira site (36.58°N, 137.60°E, elevation of 2450 m a.s.l.) of Mt. Tateyama (3015 m a.s.l.), central Japan. The first time, low molecular weight diacids, ω-oxoacids, pyruvic acid, and α-dicarbonyls were measured for this snowpit sequence. Higher concentrations of short-chain diacids (C_2-C_5) are observed in dusty snow than non-dusty snow samples. Longer chain diacids (C_7-C_{12}) are significant in granular and dusty snow samples. Aromatic and aliphatic unsaturated diacids showed higher concentrations in the slightly dusty layer deposited in winter. Except for a clean layer, molecular distributions of diacids are characterized by the predominance of oxalic acid (C_2, ave, 20±22 ng/g-snow) followed by succinic (C_4, 7.2±5.9 ng/g -snow), and malonic acids (C_3, 3.3±2.9 ng/g -snow) for all the snow layers. Lower C_3/C_4 ratios (0.46) suggest that organic aerosols are rather fresh without serious photochemical aging during the long-range transport over central Japan. The higher concentrations of the secondary species in dusty snow than non-dusty samples were mainly attributed to the heterogeneous reaction. The strong correlations of incloud oxidation products of isoprene, aromatic acids, and fatty acids suggest that condensation, oxidation, and photolysis are important reaction mechanisms for the formation of diacids. Chinese Loess (Kosa particles) and Mongolian Gobi desert's dust provided the surface area for polar organic compounds, traveled to several thousand kilometers in the lower troposphere, and snow metamorphism altered the chemical composition of diacids and related compounds.

(words: 245)

1. Introduction

Organic aerosols are characterized by an enrichment of water-soluble dicarboxylic acids (diacids) and related compounds, which includes short-chain diacids (C_2-C_5; S-DCAs) and long-chain diacids (C_6-C_{12}; L-DCAs), ω-oxoacids (ωC_2-ωC_9), pyruvic acid (Pyr), and α-dicarbonyls, i.e., glyoxal and methylglyoxal (Kawamura et al., 1996; Kunwar et al., 2017, 2019). These polar organic acids are ubiquitous in the micro scale of the lower troposphere and encompass an important fraction of fine aerosols (Liu et al., 2017, 2018, 2019; Kunwar et al., 2019). These are emitted from human activities and natural sources, i.e., primary emissions and photochemical oxidation of volatile organic compounds (VOCs) (Paulot et al., 2011; Wang et al., 2018). Terrestrial higher plants to marine phytoplanktons emitted huge amounts of biogenic VOCs, which are 10 times larger than anthropogenic VOCs on a global scale (Seinfeld and Pandis, 1998). Biogenic and anthropogenic VOCs are oxidized in the atmosphere to result in secondary organic aerosols (SOA), which are further oxidized to diacids, oxoacids, glyoxal, and methylglyoxal via heterogeneous reactions (Talbot et al., 1995; Lim et al., 2005; Volkamer et al., 2009; Kunwar and Kawamura, 2014a,b; Pokhrel et al., 2019).

Carlton et al. (2006, 2007) and Zhu et al. (2015) reported that primary organic aerosols (POA) are emitted from plants, fungal spore, fossil fuel combustion, biomass burning, and soil particles, whereas SOA are photochemically produced by heterogeneous oxidations of biogenic and anthropogenic VOCs (Surratt et al., 2010; Ho et al., 2010; Kundu et al., 2010). POA and SOA control the physicochemical properties of atmospheric particles (Kanakidou et al. 2005; Quinn and Bates, 2011), which are involved with geochemical cycles of carbon in the lower troposphere and stored in ice crystal in cold regions after snowfall (Pokhrel et al., 2015, 2020).

However, the studies on organic compounds in snow/ice archives suggested that organic compounds in snow/ice/glaciers are of biological origin (Domine et al., 2011; McNeill et al. 2012; Jacobi et al., 2012; Pokhrel, 2015; Feng et al., 2018). For example, formate and acetate using the ice sheet in Dome C from Antarctica have been reported (Saigne et al., 1987). Similarly, Kawamura et al. (1996a, 2001a,b) reported mono- and/or di-carboxylic acids in rain and snow samples from Los Angeles and Greenland ice core. Formic and acetic acids are reported from the High Mountain site (Paulot et al., 2011; Kawamura et al., 2012) and east Antarctica (de Angelis et al., 2007).

However, little is known about diacids, oxoacids, and α-dicarbonyls for different types of snow particles in the outflow regions of East Asia, in which long-range atmospheric transport is significant over the western North Pacific including Japanese Islands (Myriokefalitakis et al., 2011). Here, we report, for the first time, the molecular distribution of

86 homologous series of diacids and related compounds in different types of snow samples
87 collected from snow pit (6.5 m depth) at a high mountain site in central Japan. Besides, we
88 compare the diacids compositions of this snowpit sequence with reference dust collected from
89 the Gobi desert, Tengger, and Chinese loess plain (Fig. 1).

90 **2. Samples and methods**

91 A series of snow pit samples (10) were obtained by cutting the snowpit wall and
92 surfaces (length 0.0-6.5) on 19 April 2008 at the Murodo Daira site (36.58° N, 137.60° E, the
93 elevation of 2450 m a.s.l), central Japan (Table S1 and Fig. 1). The snow samples were placed
94 in a pre-cleaned glass jar (8 L) with a Teflon-lined screw cap using a clean stainless steel scoop,
95 to which mercuric chloride was added to avoid microbial degradation of organic compounds.
96 These samples were transported to Hokkaido University and stored in a dark refrigerator room
97 at 4°C before analysis (Kawamura et al., 2012).

98 Low molecular weight diacids (LMW-DCAs) and related compounds, oxoacids, and α-
99 dicarbonyls were measured using the methods reported elsewhere (Kunwar and Kawamura,
100 2015). The homologous series of LMW-DCAs and related compounds, as well as fatty acids,
101 were determined using butyl ester derivatization methods (Mochida et al., 2003). Briefly, ca.
102 100 mL of snow meltwater were placed in a pear shape flask (300 mL) and the pH of the
103 sample was adjusted to 8.5-9.0 using a 0.05 M KOH solution. The samples were concentrated
104 down to ca. 5 mL using a rotary evaporator under vacuum at 50°C. The concentrates were
105 transferred to a pear-shaped flask (50 mL), concentrated until dryness using a rotary evaporator
106 under vacuum, and then reacted with ~0.25 mL of 14% boron trifluoride (BF_3)/n-butanol at
107 100°C for 1 hour. During this procedure, -COOH groups were converted to butyl esters, and
108 carbonyl groups converted to dibutoxy acetal. The butyl ester and acetal derivatives were
109 determined using capillary gas chromatography (GC; HP 6890). The GC peak identification
110 was performed using a GC/mass spectrometry.

111 Before the analysis of real snowpit samples, a recovery test was conducted. Authentic
112 standard solution (10 µl) containing free oxalic (C_2), malonic (C_3), succinic (C_4), glutaric (C_5),
113 and adipic (C_6) acids with concentrations of 1.03, 1.12, 1.46, 1.04, and 0.83 nmoles/µl,
114 respectively, was spiked to organic-free pure water (100 ml) and analyzed as a real sample.
115 The recoveries were above 89% for C_2 and more than 91% for C_3, C_4, C_5, and C_6. Similarly, C_2
116 is the most volatile organic compound among these diacids and related compounds, thus C_7 to
117 C_{12} and other compounds have more than 89%. The analytical errors (replicate) were < 6% for
118 each compound whereas laboratory blanks of LMW-diacids were < 4% of the levels of real

samples, and these all compounds are corrected for the blanks. The analyses of snow pit samples were completed in 2010.

3. Analysis of reference dust materials

Reference Chinese dust samples were provided by National Institute of Environmental Studies, Japan (e.g., Nishikawa et al., 2000, 2013). The approximate sampling sites are given in Fig. 1. The height of the sites is about 1800 m above sea level. Reference dust materials (Kosa) including Chinese loess deposits from the Tengger (CJ-1, < 250 μm and CJ-2, < 100 μm) and Mongoliyan Gobi deserts (G-D, < 10 μm) were analyzed for LMW dicarboxylic acids. Chinese loess material (CJ-1) was collected in an arid area near Ruining in Gansu Province. Simulated Asian mineral dust material (CJ-2) were collected from the southeast part of the Tengger desert in the Ningxia Hui autonomous region of China. The reference materials were purchased from the National Institute for Environmental Studies. 0.1 g of reference dust samples were extracted with ultra-pure water by the methods as described above for diacids and ions. The detailed information of reference samples is reported elsewhere (Nishikawa et al., 2000, 2013). Five day backward trajectories arriving at Murodo-Daira, Mt. Tateyama of central Japan during the snow accumulation period (2007 October to 2008 April) reach to the sampling sites of reference materials (CJ-1, CJ-2, and G-D) (Fig. 1).

4. Backward Air Mass Trajectory Analysis

Figure 1 represents cluster analysis of 5 days-backward trajectories at Murodo-Daira, Mt. Tateyama in central Japan (2007 October to 2008 April) at 2500 meters above the sea level (a.s.l.). The back trajectory analyses reveal that the source of air masses are influenced by East Asia (e.g., CJ-1, CJ-2, and G-D) via long-range atmospheric transport. Air masses were originated over the same dust region of Northwest China on 31 Dec, 11 Jan, 11 Feb. Besides, 15 April showed Northeast China, central Mongolia, and the mainland of Russia and 3 March showed the Siberian region of southeast Russia. However, the air mass origin is very short on 19 April represents short-range airmass transport Northeast China and Hokkaido, Japan (Fig. 1). Kawamura et al. (2012) has reported a detailed description of sampling method and backward trajectories at Murodo-Daira.

5. Results and Discussion

5.1. Molecular distributions of dicarboxylic acids and related compounds

Figure 2 shows the molecular distributions of diacids (DCAs), oxoacids and α-dicarbonyls for each snow pit samples from Central Japan. Among 10 samples, we found dust layers that are associated with 4 snowpit samples (sample no. 2, 6, 7, and 9), which are categorized as dusty snowpit samples. The remaining samples do not contain dust layers (sample no. 1, 3, 4, 5,

153 8, 10) and categorized as non-dusty snowpit samples. The molecular distributions of non-dusty
154 snowpit samples showed a predominance of C_2 (ave. 8.6±4.5 SD ng/g-snow) followed by C_4
155 (4.2±3 ng/g-snow), C_3 (1.9 ±1.6 ng/g-snow), and phthalic (Ph) acid (1.4±1.1 ng/g-snow).
156 Similar distributions ($C_2 > C_4 > C_3$) were observed in biomass burning aerosols and marine
157 aerosols (Kundu et al., 2010b; Cong et al., 2015; Hoque et al., 2015, Deshmukh et al., 2017;
158 Kunwar et al., 2019). The molecular distributions of dusty snowpit samples showed a
159 predominance of C_2 (12-74 ng/g-snow, ave: 37±28 ng/g-snow), followed by C_4 (3.4-18 ng/g-
160 snow, 12±7 ng/g-snow) and Ph (0.75-14 ng/g-snow, 7.2±5.9 ng/g-snow). Ph is the third most
161 abundant diacid in the dusty snowpit samples, suggesting more anthropogenic sources
162 influenced in the dusty snowpit sample during long-range atmospheric transport. Ph is reported
163 as a tracer of the anthropogenic sources (Pavuluri et al., 2010).
164 Photochemically aged aerosols in the ambient atmosphere showed that C_3/C_4 ratios are
165 higher than 2.0 (Kawamura and Bikkina, 2016; Kunwar and Kawamura, 2014a). However, the
166 concentration ratios of C_3/C_4 in the snowpit samples are less than unity (dusty snowpit: ave.
167 0.48±0.06 and non-dusty snowpit: ave. 0.40±0.14), which will be discussed in a later section
168 (section 5.3). This molecular signature infers that the organic species scavenged over the
169 snowpit site are significantly influenced by biomass/biogenic emission together with
170 anthropogenic sources without serious photochemical aging.
171 Table S2 shows the average concentrations and concentration ranges of homologous
172 series of normal saturated (C_2-C_{12}), branched-chain (iC_4-iC_6), unsaturated (M, F, mM, Ph, iPh,
173 and tPh), keto (kC_3 and kC_7) and hydroxyl (hC_4) diacids, oxocarboxylic acids (ωC_2-ωC_9 and
174 Pyr), and α-dicarbonyls (Gly and MeGly) in dusty and non-dusty snowpit samples, and
175 reference Chinese dust samples. The reference dust samples were collected from three regions
176 from East Asia; Tengger desert (CJ-1), Chinese loess (CJ-2), and Gobi desert (G-D) (Fig. 1).
177 The concentration ranges and average concentrations of C_2, C_3, and C_4 in dusty snowpit
178 samples are 12-74 ng/g-snow and ave. 37±28 ng/g-snow, 1.7-9.1 ng/g-snow and 5.6±3.2 ng/g-
179 snow, and 3.4-18 ng/g-snow and 12±7.2 ng/g-snow, respectively, whereas those in non-dusty
180 snowpit samples are 3-15 ng/g-snow and 8.6±4.5 ng/g-snow, 0.44-4.5 ng/g-snow and 1.9±1.6
181 ng/g-snow, and 1.4-7.1 ng/g-snow and 1.9 ±1.6 ng/g-snow, respectively (Table S2). The
182 concentration range of oxalic acid in non-dusty samples are comparable to those reported in
183 central Greenland ice core (range: 1-20 ng/g-ice) (Kawamura et al., 2001b). Greenland is
184 influenced by biomass burning activities (Savarino and Legrand 1998). The average
185 concentration of oxalic acid in non-dusty snowpit samples in this study (8.6±4.5 ng/g-snow) is

1.6 times lower than 180-year average of oxalate concentrations from Mt. Everest ice core (13.7 ng/g-ice ng/g-ice) (Kang et al., 2001), 4.0 times higher than Greenland Site-J (0.36-11 ng/g-ice, ave. 2.1 ng/g-ice) ice core (Kawamura et al., 2001a) but similar to those (2.0-28 ng/g-ice, ave. 7.2±4.2 ng/g-ice) from Alaskan ice core (Pokhrel, 2015). The concentration range of oxalic acids in non-dusty samples in this study is very similar to those of fresh snow collected on the route from Syowa Station to Dome Fuji Station (range: 2.17-17.4 ng/g-snow), Antarctica (e.g., Matsunaga et al., 1999; and references therein). Alaskan fine aerosol sample ($PM_{2.5}$) showed somewhat different molecular distribution ($C_2 > C_3 > C_4$) during the biomass burning periods (Deshmukh et al., 2018).

The concentrations of C_2, C_3, and C_4 in dusty snowpit samples are 4.3, 2.9, and 2.8 times higher than non-dusty snowpit samples, respectively. Aromatic diacids such as phthalic (Ph), isophthalic (iPh) and terephthalic (tPh) are more abundant in dust samples by a factor of 5, 4 and 7.5 times, respectively. Aromatic diacids (e.g., Ph) are emitted to the atmosphere by anthropogenic activities such as fossil fuel combustion, whereas tPh is emitted by the plastic burning (Kunwar and Kawamura, 2014a; Jung et al., 2010). Hence, more anthropogenic and plastic burning tracers are condensed and adsorbed on the dust surface during long-range atmospheric transport. Dust can provide the surface area for organic and inorganic acids, which can be easily traveled to several thousand kilometers in the atmosphere (Kunwar et al., 2016, 2017; Hoque et al., 2020). Glyoxylic (ωC_2), pyruvic (Pyr), glyoxal (Gly), and methylglyoxal (MeGly) are produced in the atmosphere by oxidation of the precursor compounds such as isoprene. Their concentrations in dusty snowpit samples are 3.5, 3.6, 6.6, and 5 times higher than those of non-dusty samples.

Figure 3 shows the profiles of selected DCAs in snowpit sequences (samples Nos.1 to 10). Similar profiles were found for C_2-C_5 (except for C_2 and C_4 at point Nos. 2 and 4, respectively), methylsuccinic (iC_5), maleic (M), fumaric (F), and methylmaleic (mM) acids (Fig. 3a-d). Except for C_6 (not shown in fig.), all these diacids (C_2-C_5) and related compounds showed higher concentrations with dusty snowpit samples (e.g., sample Nos. 6 and 7). In contrast, C_6 showed higher concentration in clean snow (sample No. 8). We have reanalyzed this sample to check about such a high concentration of C_6. Reanalysis showed a similar concentration. Hence, we believe that there is a specific source of C_6.

Figure 3c showed straight forward concentration trends of branched-chain saturated diacids (iC_4, iC_5, and iC_6). Among the branch chain diacids, methyl succinic acid (iC_5) is the dominant (1.25±0.95 and 0.28±0.24 ng/g-snow) branched-chain diacid in dusty and non-dusty snowpit samples. Concentration trends of branched-chain diacids are flat in sample Nos. 1 to 5

(0.0-0.50 m in depth). Branched-chain diacids are emitted by anaerobic bacteria (e.g., Allison, 1978). Thus, iso C_4-C_6 diacids could be involved with bacterial activities in the ocean surfaces, atmospheric aerosols, and soil dust. Interestingly, we also found a good correlation of iso diacids (iC_4, iC_5 and iC_6) with C_2 (R^2=0.96), C_3 (0.94), C_4 (0.98), C_5 (0.98), and suberic (C_8) acid (0.89), suggesting that short-chain (C_2-C_5) and long-chain diacids (C_8) are produced by bacterial activities before snow formation phase and incloud oxidation.

Figures 3d and 3e present the concentrations of aliphatic unsaturated and aromatic diacids in the snow sequence, respectively. They showed higher concentrations in slightly dusty snow sample (No. 7), being different from short-chain diacids such as C_2 and C_3, which showed maxima in the dust layer (No. 6). Aromatic diacids are associated with coal and plastic burning, whereas aliphatic unsaturated diacids are formed by the degradation of aromatic hydrocarbons. A considerable amount of coal is burned for heating purposes during winter in East Asia, especially in China. Thus, the higher concentrations of diacids in a slightly dusty snowpit layer (No. 7) should be involved with condensation and adsorption of coal burning-derived aerosols on dust surface and transported from the Asian continent over Mt. Tateyama in winter (Table S1).

Figure 4b-c shows the profiles of concentrations of long-chain diacids (C_7-C_{12}), oxoacids, pyruvic acid, and α-dicarbonyls. Among long-chain diacids, C_9 shows the highest concentration. Except for C_6, long-chain diacids (e.g., C_7-C_9) showed higher concentrations in surface granular (No. 3) and dusty snowpit samples during Asian dust events, whereas C_{10} to C_{12} diacids showed the highest concentration in dusty snow pit layer (Fig. 4c), followed by the second (except for C_{11}) and third peak in the clean snow (No. 8) and surface granular snow (No.3) samples. Minimum concentrations were observed in surface fresh snow (No. 1), clean snow (No. 8) samples (except for C_{10}), and/or bottom of the snowpit (No. 10). The oxidation products of low molecular weight unsaturated fatty acids (e.g., $C_{14:1}$, $C_{16:1}$, $C_{18:1}$, $C_{18:2}$, $C_{18:3}$, $C_{18:1\omega7}$, and $C_{18:1\omega9}$) derived from phytoplankton and bacterial activities and high molecular weight unsaturated fatty acids (e.g., $C_{20:4}$, $C_{20:5}$, $C_{22:1}$, $C_{22:6}$, and $C_{24:1}$) are pimelic (C_7), suberic (C_8), azelaic (C_9) sebacic (C_{10}), undecanedioic (C_{11}), and dodecandioic (C_{12}) acids (C_7-C_{12}). For example, C_9 and C_{11} can be produced by the photooxidation of unsaturated fatty acids (UFAs) such as oleic acid ($C_{18:1}$) and vaccenic acid ($C_{18:1}$ ω_7), which are primarily emitted from marine microbial activities and can be found in the sea surface microlayers (Winterhalter et al., 2009). Azelaic acid (C_9) shows the highest concentration in granular snow (sample No. 3) followed by dusty snow layer (No. 6) and lower concentrations in fresh (No. 1), clean (No. 5), and bottom of sequence snow samples (No. 10). C_9 is a specific photochemical oxidation

product of biogenic UFAs (e.g., $C_{18:1}$) (Kawamura and Gagosian, 1987) and can be further oxidized to C_6, C_7, and C_8 and short chain diacids (C_2-C_5) (Legrand et al., 2007; Pavuluri et al., 2015).

5.2. Molecular composition and concentration trends of oxoacids, pyruvic acid, and α-dicarbonyls

Among oxoacids, glyoxylic (ωC_2) acid is the dominant species (dusty snowpits: ave. 9.7 ±6.3 ng/g-snow, and non-dusty snowpits: 2.7 ±2.3 ng/g-snow), followed by 4-oxobutanoic (ωC_4) acid (2.6 ±1.6 ng/g-snow and 0.82±0.51 ng/g-snow) and 3-oxopropanoic (ωC_3) acid (1.3 ±0.84 ng/g-snow, and 0.32±0.12 ng/g-snow) in both dusty and non-dusty snow pit samples (Table S2). Oxoacids ($\omega C_2 > \omega C_4 > \omega C_3$) showed molecular characteristics similar to those of diacids ($C_2 > C_4 > C_3$). Predominance of ωC_2 and ωC_4 were reported from Antarctic aerosol samples (Kawamura et al., 1996b) and predominance of ωC_2 is reported frequently from the observation studies conducted at many sites in the world, where atmospheric oxidation of precursor compounds is an important factor (Kunwar et al., 2016, 2017, 2019, references therein). We detected high concentrations of ωC_2 in the snowpit sequence, which can be derived from the oxidation of glyoxal (Gly), methylglyoxal (MeGly), maleic (M), methylmaleic (mM) and fumaric (F) acids, aromatic hydrocarbon, and unsaturated fatty acids. On the other hand, ωC_3 and ωC_4 are oxidation products of unsaturated fatty acids and longer chain ω-oxoacids (e.g. ωC_5-ωC_9) rather than anthropogenic sources (Kawamura et al., 2001a,b; Pokhrel, 2015). ωC_2-ωC_4 show similar concentration trends to each other (Fig. 3d). These results suggest that they were co-transported and formed from similar sources during long-range atmospheric transport.

The concentrations trends of ω-oxoheptanoic (ωC_7), ω-oxooctanoic (ωC_8), and ω-oxononanoic (ωC_9) acids are similar to each other (Fig. 4e) with maxima during Asian dust periods (Nos. 6, 7, and 9). On the other hand, the lower concentrations were observed in sample No. 5 (snow with ice plate) followed by No. 3 (surface granular snow) and/or No. 1 (surface fresh snow) (Table S1 and S2). They may be derived from both anthropogenic and marine biogenic sources during long-range atmospheric transport. The higher concentrations of oxoacids in the dusty snowpit samples suggest that ω-oxoacids are emitted from biogenic sources which could be injected from the Asian dust source regions with more microbial activities via long-range atmospheric transport (Wang et al., 2017).

Incloud oxidation of isoprene (Carlton et al., 2006, 2007), aromatic hydrocarbons and/or biomass burning products (Pavuluri et al., 2010) can contribute pyruvic (Pyr) acid.

Recent studies showed that third-generation products of isoprene are methylglyoxal (MeGly) and glyoxal (Gly). MeGly and intermediate compounds, e.g., malic acid (hC_4) can be further oxidized to result in Pyr (Carlton et al., 2006, 2007). The higher concentrations of Pyr can be observed in sample Nos. 2 (dusty and granular), 6 (dusty snow layer), and 7 (slightly dusty snowpit layer).

Concentration trends of two α-dicarbonyls are similar to each other (Fig. 4f). The photochemical oxidation of aromatic hydrocarbons such as benzene, toluene, xylene and p-xylene, and alkenes produces Gly (Rogge et al., 1991, 1998; Volkamer et al., 2001, 2006). The third-generation products of isoprene, i.e., Gly and MeGly, are present in the aerosol phase (Hallquist et al., 2009). Gly and MeGly also have anthropogenic sources and can produce an end product of s-DCAs, i.e., C_2 via in-cloud aqueous phase reaction (Legrand and De Angelis, 1995; Warneck, 2003, Surrat et al., 2007) (discussed in a later section).

5.3. Relative abundances in dusty and non-dusty snowpit samples: A signal of less photochemical aging during long-range atmospheric transport

Figure 5 provides the information of the average relative abundance (%) of individual diacids in total diacids. The average relative abundance of C_2 (48%) in the dusty snowpit samples is higher than that of non-dusty samples (40%). In contrast, relative abundances C_4 and long-chain diacids (C_5-C_6) are higher in non-dusty snowpit samples. This result may suggest that the formation of short chain diacids are more significant in dusty snowpit samples from its precursors diacids. Very high relative abundance of C_2 (>80%) is the indication of gas to particle-phase conversion (Kawamura et al., 2012) as well as significant photochemical processing of long-chain diacids and aqueous phase oxidation of biogenic and anthropogenic volatile organic carbons (VOCs) via Gly, MeGly, Pyr and ωC_2 (Legrand et al., 2007; Ervens et al., 2004). An increased relative abundance of C_2 (60–70%) has been reported in the marine aerosols from the Pacific during long-range atmospheric transport (Kawamura and Sakaguchi, 1999). The relative abundances of C_2 from this study (dusty snowpit: 48% and non-dusty snowpit: 40%) are less than those reported in marine aerosols from the western Pacific (65%) (Wang et al., 2006) and the central equatorial Pacific (>70%) (Kawamura and Sakaguchi, 1999), suggesting that diacids in the snowpit samples are less aged compared to marine aerosols. The average relative abundance of ωC_2 to total oxoacids (ωC_2-ωC_9) is higher (62%) in the dusty snowpit sample than non-dusty samples (56%). Accordingly, those of ωC_4 (dusty snowpit: 18% and non-dusty snowpit: 22%) and ωC_5 (2%, and 4.2%) are higher in non-dusty samples (Fig. 5a,b).

The malonic to succinic acid (C_3/C_4) ratios have been used to evaluate the extent of photochemical aging of air masses. Low values of C_3/C_4 ratios (0.25–0.44; ave. 0.35) were reported for vehicular emissions as compared to aged atmospheric aerosols (0.6–2.9; ave. 1.6) (Kawamura and Ikushima, 1993). Malonic acid is thermally less stable than succinic acid in vehicular exhaust emissions. Lower C_3/C_4 ratios were reported in the polluted area where the primary source is significant (Kawamura and Ikushima, 1993; Deshmukh et al., 2018; Jung et al., 2010), while higher ratios were reported for aerosols collected from remote marine and remote Island (Wang et al., 2009; Fu et al., 2013; Kunwar et al., 2017). Higher C_3/C_4 ratios (0.6-5.8) has been reported from marine aerosols during round the world cruise due to the severe photochemical aging of air masses (Fu et al., 2013)**.** Similarly, higher C_3/C_4 ratios were reported in the daytime (ave. 0.81) than nighttime (0.59) samples collected from Rondonia (Brazil) (Kundu et al., 2010b) due to more photochemistry in the daytime. The average C_3/C_4 ratios from Gobi Desert (G-D), Chinese Loess (CJ-1), and Tengger dust (CJ-2) are 0.64, 0.30, and 0.46, respectively. These ratios are almost similar to this study of dusty (range: 0.50-0.51, ave. 0.50±0.00) and non-dust snowpit samples (0.23-0.63, ave. 0.41±0.14). Hence, C_3/C_4 ratios from this study indicate that dust is not responsible for the atmospheric photochemical processing of C_4 to C_3. The dominant presence of succinic (C_4) over C_3 has been reported in the Antarctic aerosols (Kawamura et al.,1996b), spring snowpack samples from the Arctic (Narukawa et al., 2002), and winter aerosols from Tokyo (Sempéré and Kawamura, 1994). It should be noted that a higher relative abundance of C_4 is common in the cold environment where photochemical oxidation is less severe (Sempere and Kawamura, 2003). The average C_3/C_4 ratio of this study is 0.46 further suggests that snow particles are influenced from urban aerosols with a strong influence of fossil fuel combustion without severe photochemical processing from transboundary air pollution of east Asia. Fresh aerosols have to be captured and deposited within the snow particles. Snow metamorphism (e.g., nos. 1 and 3) plays an important role in these diacids, i.e., fresh organic compounds are confined.

In addition, unsaturated aliphatic diacids, i.e., maleic acid (M, cis configuration) and fumaric (F, trans configuration), are formed by the degradation of aromatic hydrocarbons such as toluene and benzene in the presence of oxidants. Under the intense solar radiation, M is further isomerized to its trans isomer (F), through photochemical processes. Hence, M/F ratio can be used to better understand photoisomerization. Lower M/F ratio is deciphered to the higher photochemical aging. The M/F ratios range from 1.9-4.2 (3.0±0.8) of this study, being similar to the M/F ratios reported in the aerosols collected from remote Himalaya (1.55–8.16, ave. 4.44) (Cong et al., 2015) and urban site such as New Delhi (2.0–3.6) (Miyazaki et al.,

2009), Beijing (2.3) and Mongolia (2.0) (Jung et al., 2010). The average M/F ratio from this study is 11.5 times higher than those reported in marine aerosols collected from the North Pacific (0.26). Further, the M/F ratio of this snow samples is comparable to biomass burning aerosols from Mt. Tai, China (2.0), Rondonia, Amazonia (2.8) and Mongolia (2.0) (Kunwar and Kawamura, 2014a; Jung et al., 2010; Kundu et al., 2010b). This finding also suggests that polar organic compounds are well deposited in the seasonal climatic snow line of Mt. Tateyama. The C_3/C_4 and M/F ratios suggest that Mt.Tateyama (Fig. 1) is the receptor site of fresh aerosols at least in the winter season (end of October to April 19, 2007) of Central Japan (Table S1).

5.4. Sources and formation mechanisms of diacids in the snow samples

Phthalic acid (Ph) and terephthalic (tPh) acids are emitted to the atmosphere from polynuclear aromatic hydrocarbons (PAHs). These aromatic diacids are further degraded to M, mM, F, Gly and MeGly. These compounds further degrade to ωC_2 and finally result in oxalic acid (C_2). Hence, it is better to see the correlations between these compounds with Ph and tPh. Ph and benzoic acids show strong correlations with C_2 in the dusty (R^2= 1.00 and 1.00) and non-dusty (0.88 and 0.84) snowpit samples (Fig. S1). Further, strong correlations of Ph and benzoic acid with unsaturated aliphatic diacids such as mM in the dusty (1.00 and 0.97, respectively) and non-dusty (0.75 and 0.94) snowpit samples, F in the dusty (0.90, and 0.79) and non-dusty (0.85 and 0.94) snowpit samples. Very strong correlations of Ph and benzoic acid are observed with other descendent such as M, Gly, and MeGly in both dusty (range: 0.78 to 0.99 and 0.79 to 0.98) and non-dusty (0.42 to 0.88 and 0.84 to 0.94) snowpit samples. Similar correlations of tPh were observed with mM, C_2, ωC_2, F, M, Gly, MeGly in the dusty (0.73-0.99 and) and non-dusty (0.40-0.83) snowpit samples. This result suggests that short-chain diacids are produced by the photooxidation of aromatic hydrocarbons.

Further, both aromatic and aliphatic unsaturated diacids showed strong correlations with short-chain diacids C_2-C_5 (R^2= 0.72 to 0.99). Intermediate compounds (e.g., hC_4, kC_3, and kC_7) also showed strong correlations with C_2 (0.70, 0.77, and 0.91, respectively), C_3 (0.92, 0.82, and 0.96), C_4 (0.83, 0.85, and 0.99), and C_5 (0.82, 0.88, and 0.98). The strong correlations of C_2-C_5 diacids with unsaturated aliphatic, branched-chain and multifunctional diacids, together with tracers of plastic burning products such as Ph and tPh, suggest a contribution of anthropogenic sources including plastic burning followed by severe photochemical oxidation of PAHs and deposition to alpine snows in central Japan via long-range atmospheric transport.

Coal-burning emits sulfur dioxide (SO_2). When SO_2 reacts with water, it forms sulfuric acid (H_2SO_4) and deposits as sulfate (SO_4^{2-}). We found strong correlations of nss-SO_4^{2-} with

short chain diacids C_2-C_5 (0.53-0.79), branched saturated diacids, i.e., iC_5-iC_6 (0.73-0.74), aliphatic unsaturated diacids (0.60-0.77), aromatic diacids (0.80-0.81) and oxoacids such as ωC_2 (0.91), ωC_3 (0.53), ωC_8 (0.69), ωC_9 (0.80), benzoic acid (0.76) and MeGly (0.92) in non-dusty snowpit samples, suggesting that diacids and related compounds are linked to anthropogenic activities. ss-SO_4^{2-} is the indicator of marine source, which also showed significant correlations with oxoacids ωC_9 (0.63), ωC_8 (0.53), ωC_7 (0.57), and ωC_2 (0.65), suggesting the unsaturated fatty acids (UFAs) acids from marine source influence the non-dusty snowpit samples. UFAs acids are precursors compounds for oxoacids. These results suggest that this sampling site during the non-dust period is influenced by both marine and continental sources.

Malonic (C_3) is hardly produced by the oxidation of aromatic structures having conjugated double bonds. It is likely produced by the oxidation of succinic acid (C_4) via an intermediate compound (i.e., malic acid). C_4 can be produced from gaseous aliphatic carboxylic acids, n-alkanes, aldehydes, and mid-chain ketocarboxylic acids (Kawamura and Ikushima, 1993; Kunwar et al., 2017, 2019). Strong correlations of C_4 with hC_4 (R^2=0.91), C_3 (0.88) and C_2 (0.79) in non-dusty snowpit samples and very strong correlations of C_4 with hC_4 (0.99), C_3 (0.99) and C_2 (0.97) observed in dusty snowpit samples suggest that shorter-chain diacids are formed by the oxidation of longer-chain diacids.

nss-Ca^{2+} is a tracer of dust (Kunwar and Kawamura, 2014a). Interestingly, we found very strong correlations of nss-Ca^{2+} with C_2, (R^2= 0.98) C_3 (0.99), C_4 (0.99), and C_5 (1.00), C_7 (0.74), C_8 (0.81), C_{10} (0.99), C_{12} (0.99), iC_4-iC_5 (range: 0.92–0.99), aliphatic and aromatic acids (0.97-1.00), multifunctional diacids such as hC_4 (0.99), kC_3 (0.99), kC_7 (0.97), ω-oxoacids from ωC_2 to ωC_9 (0.92-0.99), and α-dicarbonyls such as Gly (0.98), and MeGly (0.99). The strong correlations of nss-Ca^{2+} with diacids and related compounds suggest that dust particles provided the surface for the oxidative reaction. Interestingly, nss-Ca^{2+} doesn't show any correlation with C_9 (R^2= 0.28). The strong correlations of nss-Ca^{2+} with C_8, C_{10}, and C_{12} suggest that bacterial activities from the dust are the source of long-chain diacids (Grosjean et al., 1978). Bacterial emission and unsaturated fatty acids from marine and terrestrial plants could be the precursors for C_8, C_{10}, and C_{12} diacids. A strong correlation (0.94) is observed between MSA^- and nss-Ca^{2+}, suggesting that dust is the source of MSA^-. The higher concentrations of MSA^- and the secondary species in dusty snowpit samples than non-dusty samples were mainly attributed to the heterogeneous reaction and mixing of dust with polluted aerosol.

421 **5.4. Incloud oxidation for the formation of diacid and related compounds**

422 Isoprene accounts for more than half of non-methane volatile organics globally and has
423 been proposed as the source for the production of oxalic acid in-cloud process (Warneck, 2003,
424 Lim et al., 2005). Isoprene oxidation in gas phase yields glycolaldehyde, glyoxal, and
425 methylglyoxal, which can further dissolve in water and react with OH radicals to form oxalic
426 acid via glycolic, glyoxylic, pyruvic, and acetic acids (Pokhrel, 2015, references therein). The
427 aqueous-phase chemical mechanism proposed by Lim et al. 2005 is very similar to the cloud
428 photochemistry model reported by Ervens et al. (2004) except for the fate of methylglyoxal.
429 The incloud oxidation model proposed by Ervens et al. (2004) is the reaction between
430 methylglyoxal and OH, which yields pyruvic acid that is further oxidized to acetaldehyde and
431 finally CO_2 without forming low-volatility organic acids. However, methylglyoxal oxidation
432 yields pyruvic, acetic, glyoxylic, and finally oxalic acids (Lim et al., 2005). We found very
433 strong correlations (R^2) of C_2 with its precursor compounds (except for sample no. 6) such as
434 ωC_2 (dusty snowpit samples: 0.95 and non-dusty samples: 0.84), Gly (1.00 and 0.28), Pyr (0.70
435 and 0.16), and MeGly (0.99 and 0.82) (Fig. S1). However, C_2 does not show any correlations
436 with formic (0.00) and acetic (0.01) acids, but shows a strong correlation (0.70) with suberic
437 (C_8) acid in dusty snowpit samples (Fig. S2). Hence, hydrated glyoxylic acid is the major
438 pathway for the formation of oxalic acid in the cloud. Field observation from this sampling site
439 is similar to the in-cloud oxidation model of isoprene proposed by Ervens et al. (2004). For the
440 correlation analysis of dust samples, we did not include sample no. 6, which showed very high
441 concentrations of these diacids and related compounds (i.e., Fig. S1, S2, and S3).

442 Aromatic hydrocarbons (benzene and toluene) are the main suppliers of anthropogenic
443 emissions. Among these, toluene is one of the most ample species in the atmosphere. The
444 average concentrations of toluene were reported to be 2–39 ppb in urban, 0.05–0.8 ppb in rural,
445 and 0.01–0.25 ppb in remote areas (Finlayson-Pitts and Pitts, 2000). Aromatic hydrocarbons
446 are oxidized in the presence of OH, forming glyoxal and methylglyoxal. They have thus
447 formed Gly and MeGly, which are further oxidized by the OH radicals or decayed by
448 photolysis. Due to their highly effective Henry's law constants (i.e., including hydration of the
449 aldehydes), significant amounts of both glyoxal and methylglyoxal are dissolved in cloud water.
450 Additional oxidation products include ring retaining products (e.g., benzaldehyde, benzoic
451 acids), which can also partition into the aerosol surface, thus contributing to secondary organic
452 aerosol mass (Odum et al., 1996). Interestingly, phthalic acid (Ph) showed a strong correlation
453 with Gly (dusty snowpit samples: 0.99 and non-dusty samples: 0.42) and MeGly (1.00 and
454 0.81). In addition, Ph showed strong correlations with mM (1.00 and 0.75), F (0.99 and 0.85),

M (1.00 and 0.79), and C_2 (1.00 and 0.88). Benzoic acid also showed strong correlation with mM (0.99 and 0.94), F (0.99 and 0.94), M (0.99 and 0.94), Gly (1.00 and 0.94), MeGly (0.99 and 0.94), and C_2 (1.00 and 0.84) (Fig. S3).

The occurrence of normal short-chain diacids (C_2-C_5), Pyr, Gly, MeGly and long-chain diacids (C_8, C_{11}, C_{12}), oxoacids, aromatic diacids, and their precursors compounds together with correlation analysis (Fig. S2 and S3) suggest that dust and non-dust samples emitted in the source region and mixed with the polluted air during the long-range atmospheric transport. Snow essentially comes from cloud water. Hence, incloud oxidation of isoprene, aromatic acids, fatty acids, and bacterial metabolisms activities are an important source for diacids in snowpit samples. Hence, heterogeneous oxidation reactions within the cloud condensation, oxidation, and photolysis are the main reactions that took place in the cloud before reaching the sampling site.

5.5. Concentration ratios in dusty and non-dusty snowpit samples: A link to more anthropogenic activities in dusty snowpit samples

Ph is produced by incomplete combustion of PAHs such as naphthalene, whereas the incomplete combustion of cyclic olefins (e.g., cyclic hexene) produces C_6. In contrast, C_9 is a specific oxidation product of biogenic unsaturated fatty acids having a double bond at C_9 position. Hence, Ph/C_9 and C_6/C_9 ratios have been used as tracers to better distinguish anthropogenic versus biogenic emissions (Pavuluri et al., 2010). The Ph/C_9 (dust: 8.0 and non-dust: 2.3) and C_6/C_9 (2.0 and 1.3) ratios are higher in dusty snowpit samples, suggesting that dust provided the surface area to adsorb anthropogenic organic compounds during the long-range atmospheric transport (Kunwar and Kawamura, 2014a,b). The biogenic volatile organic compounds (BVOCs) such as isoprene may be oxidized in the atmosphere to form less volatile compounds that may condense and contribute to SOA formation (Kunwar et al., 2014a). Biogenic emissions contribute more production of MeGly than Gly, giving higher of MeGly/Gly ratios. We found that MeGly/Gly (0.39 and 0.52) ratios are higher in non-dusty snowpit samples, further suggesting less biogenic influence in dusty snowpit samples.

C_2 is formed by the oxidation of long-chain diacids such as C_9. Hence, C_2/C_9 ratios can decipher the formation of low molecular diacids from long-chain diacids. C_2/C_9 (42 and 14) ratios are higher in dusty snowpit samples, suggesting that an intensive degradation of longer-chain diacids occurs on the dust surface during long-range atmospheric transport because dust provides a favorable area for the chemical reaction. The elevation of 2450 m a.s.l. of this sampling site lies below the climatic snow line (Mt. Tateyama: 36.58° N), which is similar to the elevation of climatic snow line (ground temperature below 0°C) of Eastern Siberia (2300-

2800 m), Kamchatka interior (2000-2800 m), northern slopes of Alps (2500-2800 m), and Rocky Mountains (2100-3350 m) in the Northern Hemisphere (*https://nsidc.org and https://www.quora.com*). Thus, snowfalls in Mt. Tateyama well captured these polar organic compounds, demonstrating that the heterogeneous aqueous reactions occur before the snow formation phase in the troposphere during the cold months from November-April via a long-range atmospheric transport of Asian Dust at high altitude over central Japan.

6. Summary and Conclusions

We study, for the first time, water-soluble dicarboxylic acids and related compounds in snow pit samples collected from the Alpine mountain site in central Japan (elevation, 2450 m a.s.l.). The molecular distributions of diacids are characterized by the predominance of oxalic acid (C_2) followed by succinic acid (C_4) and phthalic (Ph) in dusty snowpit samples (C_2>C_4>Ph), whereas malonic (C_3) acid is predominant after C_4 in the non-dusty snowpit samples (C_2>C_4>C_3). Glyoxylic (ωC_2) acid is the most abundant oxoacid followed by 4-oxobutanoic (ωC_4) and 3-oxopropanoic (ωC_3) acid for dusty and non-dusty snowpit samples. The molecular characteristics are consistent between oxoacids (ωC_2>ωC_4) and diacids (C_2>C_4), suggesting that organic compounds in snowpit sequences have a similar photochemical process and/or similar source. The C_3/C_4 ratios of Gobi desert (0.30), Chinese Loess (0.30), and Tengger dust (0.46) are close to this study of non-dusty (range: 0.22 to 0.63, ave. 0.41±0.14), dusty (0.50 to 0.51, ave. 0.50±0.007), and total samples (n=10) of snowpit (0.23-0.63, ave. 0.45 ±0.12), indicating the influence of fresh aerosols prior to the formation of snow particles.

The relative abundance of C_2 (48%) to total diacids is higher in dusty snowpit samples, suggesting that the aerosols are subjected to more photochemical oxidation for dusty samples. We found very strong correlations (R^2) of C_2 with its precursors such as ωC_2 (dusty snowpit samples: 0.95 and non-dusty snowpit samples: 0.84), Gly (1.00 and 0.28), MeGly (0.99 and 0.82), Pyr (0.70 and 0.16) and suberic acid (0.70 and 0.50). Hence, hydrated glyoxylic acid is the major pathway for the formation of oxalic acid via heterogenous incloud oxidation. The C_6/C_9 (dusty snowpit samples: 2.0, non-dusty snowpit samples: 1.27), Ph/C_9 (8.0 and 2.3), and C_2/C_9 (41.6, 14.0) ratios are higher in dusty snowpit layers, suggesting the mixing of polluted air masses with the dusty aerosols followed by snow scavenging.

We found very strong correlations of nss-Ca^{2+} with short-chain diacids, i.e., C_2, C_3, C_4, and C_5 (range: 0.98-1.00), long-chain diacids, e.g., C_7 (0.74), C_8 (0.81), C_{10} (0.99), C_{12} (0.99), iC_4-iC_5 (0.92-0.99), aliphatic and aromatic acids (0.97-1.00), multifunctional diacids such as hC_4 (0.99), kC_3 (0.99) and kC_7 (0.97), ω-oxoacids from ωC_2 to ωC_9 (0.92-0.99), Gly (0.98),

522 and MeGly (0.99), suggesting that dusts provide the surface for the oxidative reaction. Snow
523 particles essentially come from cloud water (>2000m). Hence, the strong correlations of
524 incloud oxidation product of isoprene, aromatic acids, and fatty acids suggest heterogeneous
525 aqueous phase reaction together with adsorption, condensation and photolysis and/or in situ
526 oxidation processes are an important source for diacids and related compounds and they are
527 involved in cloud condensation nuclei and well deposited in the sampling site of Mt. Tateyama
528 (2450m a.s.l.), sea coast in central Japan. It further helps to evaluate air quality in the free
529 troposphere during cold months of central Japan (November-April), showing the atmospheric
530 transport and formation processes of organic compounds in dusty and non-dusty snow layers,
531 and diacids photochemistry during snow metamorphism.
532
533 **Acknowledgments**

534 This study was, in part supported by the Japan Society for the Promotion of Science
535 through Grant-in-Aid No. 24221001 and Japan Student Services Organization (JASSO).
536 (Total words: 6,489)
537
538 **References**

539 Allison, M.J. Production of branched-chain volatile fatty acids by certain anaerobic bacteria. Applied and
540 Environmental Microbiology. 1978, 35 (5) 872-877, doi: 0099-2240/78/0035-0872.
541 Carlton, A.G.; Barbara, J.T; Lim, H.J.; Altieri, E.K.; Seitzinger, S. Link between isoprene and secondary organic
542 aerosol (SOA): Pyruvic acid oxidation yields low volatility organic acids in clouds. J. Geophys. Res. Lett.
543 2006, 33, L06822, doi: 10.1029/2005GL025374.
544 Carlton, A.G.; Turpinb, B.J.; Altieric, K.E.; Seitzingerc, S.; Reffd, A.; Lime, H.J.; Ervens, B. Atmospheric oxalic
545 acid and SOA production from glyoxal: Results of aqueous photooxidation experiments. Atmos. Environ.
546 2007, 41, 7500-7602.
547 Cong, Z.; Kawamura, K.; Kang, S.; Fu, P. Penetration of biomass-burning emissions from South Asia through the
548 Himalayas: new insights from atmospheric organic acids. Scientific Reports, 2015, 5, 9580, doi:
549 10.1038/srep09580.
550 de Angelis, H.; Kleman, J. Palaeo-ice streams in the Foxe/Baffin sector of the Laurentide Ice Sheet. Quaternary
551 Science Rev. 2007, 26, 1313–1331.
552 Deshmukh, D.K.; Kawamura, K.; Lazaar, M.; Kunwar, B.; Boreddy, S. K. R. Dicarboxylic acids, oxoacids,
553 benzoic acid, α-dicarbonyls, WSOC, OC, and ions in spring aerosols from Okinawa Island in the western
554 North Pacific Rim: Size distributions and formation processes. Atmos. Chem. Phys., 2016, 16, 5263–5282.
555 Deshmukh, D.; Kawamura,K.; Deb, M.; Boreddy, S.K.R. Sources and formation processes of water-soluble
556 dicarboxylic acids, ω-oxocarboxylic acids, α-dicarbonyls, and major ions in summer aerosols from eastern
557 central India. J. Geophys. Res.-Atmos. 2017, 122, 3630-3652, doi: 10.1002/2016JD026246.
558 Deshmukh, D.K.; Kawamura, K.; Haque, Md. M.; Kim, Y. Dicarboxylic acids, oxocarboxylic acids and α-
559 dicarbonyls in fine aerosols over central Alaska: Implications for sources and atmospheric processes. Atmos.
560 Res. 2018, 202 128- 139.
561 Domine, F.; Charles, G.J.; Barret, M.; Houdier, S.; Voisin, D.; Douglas, TA.; Blum, J.D.; Beine, H.J.; Anastasio,
562 C.; François-Marie, B. The specific surface area and chemical composition of diamond dust near Barrow,
563 Alaska. J. Geophys. Res. 2011, 116, D00R06, doi: 10.1029/2011JD016162.
564 Ervens, B.; Feingold, G.; Clegg, S.L.; Kreidenweis, S.M. A modeling study of aqueous production ofdicarboxylic
565 acids: 2. Implications for cloud microphysics. J. Geophys. Res. 2004,109, D15206,
566 doi:10.1029/2004JD004575.
567 Ervens, B.; Feingold, G.; Frost, G.J.; Kreidenweis, S.M.; A modeling study of aqueous production of dicarboxylic
568 acids, 1. Chemical pathways and speciated organic mass production. J., Geophys. Res. 2004, 109, D15205,
569 doi: 10.1029/2003JD004387.

570 Feng, L.; An, Y.; Xu, J.; Kang, S.; Characteristics and sources of dissolved organic matter in a glacier in the
571 northern Tibetan Plateau: Differences between different snow categories. Annals of Glaciology. 2018, 1-10,
572 doi:10.1017/aog.2018.20
573 Finlayson-Pitts, B.J.; Pitts, J.N. Chemistry of the Upper and Lower Atmosphere. Academic Press, San Diego.
574 2000, 8, 294-348, doi: 10.1016/B978-012257060-5/50010-1.
575 Fu, P.; Kawamura, K.; Usukura, K. Miura, K. Dicarboxylic acids and related polar compounds in the marine
576 aerosols collected during a round-the-world cruise. Marine Chemistry. 2013, 148, 22-32.
577 Grosjean, D.; Cauwenberghe, K.V.; Schmid, J.P.; Kelley, P.E.; Jr. Pitts, J.N. Identification of C_3 - C_{10} aliphatic
578 dicarboxylic acids in airborne particulate matter. Environ. Sci. & Technol. 1978, 12, 313 -317.
579 Hallquist, M.; Wenger, J.C.; Baltensperger, U. The formation, properties and impact of secondary organic
580 aerosol:current and emerging issues. Atmos. Chem. Phys. 2009, 9, 5155-5235.
581 Hoque, M. Md. M.; Kawamura, K.; Nagayam, T.; Kunwar, B.; Peltzer, E.T.; Gagosian, R.B. Molecular
582 characteristics of water-soluble dicarboxylic acids, ω-oxocarboxylic acids, pyruvic acid and α-dicarbonyls in
583 the aerosols from the eastern North Pacific. Marine, Chem. 2020, 103812.
584 Ho, K. F.; Lee, S.C.; Ho, S.S.H.; Kawamura, K.; Tachibana, E.; Cheng, Y.; Zhu, T. Dicarboxylic acids,
585 ketocarboxylic acids, α-dicarbonyls, fatty acids, and benzoic acid in urban aerosols collected during the 2006
586 Campaign of Air Quality Research in Beijing (CAREBeijing‐2006). J. Geophys. Res. 2010, 115, D19312,
587 doi: 10.1029/2009JD013304.
588 Hoque, M.; Kimitaka, k.; Osamu, S.; Hoshi, N. Spatial distributions of dicarboxylic acids, ω-oxoacids, pyruvic
589 acid and α-dicarbonyls in the remote marine aerosols over the North Pacific. Mar. Chem. 2015, 172, 1-11.
590 Jacobi, H.W.; Voisin,D.; Jaffrezo, J.L.; Cozic, J.; Douglas, T.A.; Chemical composition of the snow pack during
591 the OASIS spring campaign 2009 at Barrow, Alaska. J. Geophys. Res. 2012, 117, D00R13,
592 doi:10.1029/2011JD016654.
593 Jung, J.; Tsatsral, B.; Kim, Y.J.; Kawamura, K. Organic and inorganic aerosol compositions in Ulaanbaatar,
594 Mongolia, during the cold winter of 2007 to 2008: Dicarboxylic acids, ketocarboxylic acids, and
595 α–dicarbonyls. J. Geophys. Res. 2010, doi.org/10.1029/2010JD014339.
596 Kanakidou, M.; Seinfeld, J.H.; Pandis, S.N.; Barnes, I.; Dentener, F. J.; Facchini, M.C.; Dingenen, R.V.; Ervens,
597 B.; Nenes, A.; Nielsen, C.J.; Swietlicki, E.; Putaud, J.P.; Balkanski, Y.; Fuzzi, S.; Horth, J.; Moortgat, G.K.;
598 Winterhalter, R.; Myhre, C.E.L.; Tsigaridis, K.; Vignati, E.; Stephanou, E.G.; Wilson, J. Organic aerosol and
599 global climate modelling: a review. Atmos. Chem. and Phys. 2005, 5, 1053e1123.
600 Kang, S.; Qin, D.; Mayewski, P.A.; Wake, C.P. Recent 180 years of oxalate recovered from a Mt. Everest ice core
601 and environmental implications. J. of Glacio. 2001, 47 (156), 155-156.
602 Kawamura K.; Yokoama,K.; Fujii, Y.; Watanabe, O. A Greenland ice core record of low molecular weight
603 dicarboxylic acids, ketocarboxylic acids, and dicarbonyls: A trend from Little Ice Age to the present (1540 to
604 1989A.D.), J. Geophys. Res. 2001b, D1(106), 1331-1345.
605 Kawamura, K.; Bikkina, S. A review of dicarboxylic acids and related compounds in atmospheric aerosols:
606 Molecular distributions, sources and transformation. Atmos. Res. 2016, doi: 10.1016/j.atmosres.2015.11.018.
607 Kawamura, K.; Ikushima, K. Seasonal changes in the distribution of dicarboxylic acids in the urban atmosphere,
608 Env. Sci. Tech. 1993, 27, 2227-2235.
609 Kawamura, K.; Matsumoto, K.; Tachibana, E.; Aoki, K. Low molecular weight (C_1-C_{10}) monocarboxylic acids,
610 dissolved organic carbon and major inorganic ions in alpine snow pit sequence from a high mountain site,
611 central Japan. Atmos. Environ. 2012, 62, 272-280.
612 Kawamura, K.; Sakaguchi, F. Molecular distribution of water soluble dicarboxylic acids in marine aerosols over
613 the Pacific Ocean including tropics. J. Geophys. Res. 1999b, 104(D3), 3501–3509, doi:
614 10.1029/1998JD100041.
615 Kawamura, K.; Sempere, R.; Imai, Y.; Hayashi, M.; Fujii, Y. Water soluble dicarboxylic acids and related
616 compounds in the Antarctic aerosols. J. Geophys. Res. 1996b, 101, 18, 721-18,728 .
617 Kawamura, K.; Sempere, R.; Imai, Y.; Hayashi, M.; Fujii, Y. Water soluble dicarboxylic acids and related
618 compounds in the Antarctic aerosols. J. Geophys. Res.1996b, **101** , No. D13, 18,721-18,728 .
619 Kawamura, K.; Steinberg, S.; Ng, L.; Kaplan, I.R. Wet deposition of low molecular weight mono- and di-
620 carboxylic acids, aldehydes and inorganic species in Los Angeles. Atmos. Environ. 2001a, 35, 3917-3926.
621 Kawamura, K.; Suzuki, I.; Fujii, Y.; Watanabe, O. Ice core record of fatty acids over the past 450 years in
622 Greenland. Geophys. Res. Lett. 1996a, 23, 2665-2668.
623 Kundu, S.; Kawamura, K.; Andreae, T.W.; Hoffer, A.; Andreae, M.O. Molecular distributions of dicarboxylic
624 acids, ketocarboxylic acids and α-dicarbonyls in biomass burning aerosols: implications for photochemical
625 production and degradation in smoke layers. Atmos. Chem. Phys. 2010b, 10, 2209–2225.
626 Kundu, S.; Kawamura, K.; Lee. M. Seasonal variations of diacids, ketoacids and α-dicarbonyls in marine aerosols
627 at Gosan, Jeju Island: Implications for their formation and degradation during long-range transport. J.
628 Geophys. Res. 2010a, 115, D19307, doi: 10.1029/2010JD013973.

629 Kunwar, B.; Kawamura, K. One-year observations of carbonaceous and nitrogenous components and major ions
630 in the aerosols from subtropical Okinawa Island, an outflow region of Asian dusts. Atmos. Chem. Phys.
631 2014b, 14, 1819-1836, doi: 10. 5194/acp-14-1819-2014.
632 Kunwar, B.; Kawamura, K. Seasonal distributions and sources of low molecular weight dicarboxylic acids, ω-
633 oxocarboxylic acids, pyruvic acid, α-dicarbonyls and fatty acids in ambient aerosol from subtropical Okinawa
634 in the western Pacific Rim. Environ. Chem. 2014a, 11, 673-689.
635 Kunwar, B.; Torii, K.; Zhu, C.; Fu, P.; Kawamura, K. Springtime variations of organic and inorganic constituents
636 in sub micron aerosols (PM1.0) from Cape Hedo, Okinawa. Atmos. Environ. 2016, 130, 84-94.
637 Kunwar, B.; Torii, K.; Zhu, C.; Kawamura, K. Springtime influences of Asian outflow and photochemistry on the
638 distributions of diacids and oxoacids and α-dicarbonyls in the aerosols from the western North Pacific rim.
639 Tellus B. 2017, 69, 1369341, doi: org/10.1080/16000889.
640 Kunwar,B.; Kawamura, K.; Fujiwara, S.; Fu, P.; Miyazaki, Y.; Pokhrel, A. Dicarboxylic acids, oxocarboxylic
641 acids and α-dicarbonyls in atmospheric aerosols from Mt.Fuji, Japan: Implication for primary emission versus
642 secondary formation. Atmos. Res. 2019, 221, 58-79.
643 Legrand, M.; de Angelis, M. Origins and variations of light carboxylic acids in polar precipitation. J. Geophys.
644 Res. 1995, doi: 10.1029/94JD02614.
645 Legrand, M.; Preunkert, S.; Oliveira, T. Pio, C.A.; Hammer, S.; Gelencser, A.; Kasper-Giebl, A.; Laj, P. Origin of
646 C_2 - C_5 dicarboxylic acids in the European atmosphere inferred from year round aerosol study conducted at a
647 west-east transect. J. Geophys. Res. 2007, 112, doi: 10.1029/2006jd008019.
648 Li, X.; Jiang, L.; Bai, Y.; Yang, Y.; Liu, S.; Chen, X.; Xu, J.; Liu, Y.; Wang, Y.; Guo, X.; Wang, Y.; Wang, G.
649 Wintertime aerosol chemistry in Beijing during haze period: Significant contribution from secondary
650 formation and biomass burning emission. Atmos. Res. 2019, 218, 25-33,
651 doi.org/10.1016/j.atmosres.2018.10.010.
652 Lim, H.J.; Annmarie, G.C., Turpin, B.J. Isoprene forms secondary organic aerosol through cloud processing:
653 Model simulation. Env. Sci. Tech. 2005, 39, 4441-4446.
654 Liu, H.; Kawamura, K.; Kunwar, B.; Cao, J.; Zhang, J.; Zhan, C.; Zheng, J.; Yao, R.; Liu, T.; Liu, X.; Xiao, W.
655 Sources and formation processes of short-chain saturated diacids (C_2–C_4) in inhalable particles (PM_{10}) from
656 Huangshi City, Central China. Atmosphere. 2017, 8(11), 213: doi.org/10.3390/atmos8110213.
657 Liu, H.K.; Kawamura, K.; Kunwar, B.; Cao, J.; Zhang, J.; Zhan, C.; Zheng, J.; Yao, R.; Liu, T.; Xiao, W.
658 Dicarboxylic acids and related compounds in fine particulate matter aerosols in Huangshi, central China.
659 Journal of the Air & Waste Management Association. 2018, doi: 10.1080/10962247.2018.1557089.
660 Matsunaga, S.; Kawamura, K.; Yamamoto, Y.; Azuma, N.; Fujii, Y.; Motoyama, H. Seasonal changes of low
661 molecular weight dicarboxylic acids in snow samples from Dome-Fuji, Antarctica. Polar Meteor. and Glac.
662 1999, 13, 53-63.
663 McNeill, V.F.; Grannas, A.M.; Abbatt, J.P.D.; Ammann, M.; Ariya, P.; Bartels-Rausch, T.; Domine, F.;
664 Donaldson, D.J.; Guzman, M.I.; Heger, D.; Kahan, T.F.; Klan, K.; Masclin, S.; Toubin, C.; Voisin, D.
665 Organics in environmental ices: sources, chemistry, and impacts. Atmos. Chem. Phys. 2012, 12, 9653–9678,
666 doi: 10.5194/acp-12-9653-2012.
667 Miyazaki, Y.; Aggarwal, S.G.; Singh, K.; Gupta, P.K.; Kawamura, K. Dicarboxylic acids and water-soluble
668 organic carbon in aerosols in New Delhi, India in winter: Characteristics and formation processes. J. Geophys.
669 Res. 2009, 114, D19206, doi: 10.1029/2009JD011790.
670 Mochida, M.; Kawamura, K.; Umemoto, K.; Kobayashi, M.; Matsunaga, S.; Lim, H.; Turpin, B.J.; Bates, T.S.;
671 Simoneit, B.R.T. Spatial distributions of oxygenated organic compounds (dicarboxylic acids, fatty acids, and
672 levoglucosan) in marine aerosols over the western Pacific and off coasts of East Asia: Continental outflow of
673 organic aerosols during the ACE-Asia campaign. J. Geophys. Res. 2003, 108, D23, 8638, doi:
674 10.1029/2002JD003249.
675 Myriokefalitakis, S.; Tsigaridis, K.; Mihalopoulos, N.; Sciare, J.; Nenes, A.; Kawamura, K.; Segers, A.;
676 Kanakidou, M. In-cloud oxalate formation in the global troposphere: A 3D modeling study. Atmos. Chem.
677 Phys. 2011, 11, 5761-5782.
678 Narukawa, M.; Kawamura, K.; Li, S.-M.; Bottenheim, J.W. Dicarboxylic acids in the arctic aerosols and
679 snowpacks collected during ALERT2000, Atmospheric Environment. 2002, 36, 2491-2499.
680 Nishikawa, M.; Batdor, D.; Ukachi, M.; Onishi, K.; Nagan, K.; Mori, I.; Matsui, I.; Sano, T. Preparation and
681 chemical characterisation of an Asian mineral dust certified reference material. Analytical Methods. 2013, 5,
682 4088-4095, doi: 10.1039/C3AY40435H.
683 Nishikawa, M.; Hao, Q.; Morita, M. Preparation and evaluation of certified reference materials from Asian
684 mineral dust, Global Environ. Res. 2000, 4, 103–113.
685 Odum, J. R.; Hoffmann, T.; Bowman, F.; Collins, D.; Flagan, R. C.; Seinfeld, J. H. Gas/particle partitioning and
686 secondary organic aerosol yields. Environ. Sci. Technol. 1996, 30, 2580-2585.
687 Paulot, F.; Wunch, D.; Crounse, J.D.; Toon, G.C.; Millet, B.D.; DeCarlo, P.F.; Vigouroux, C.; Deutscher, N.M.;
688 Abad, G.G.; Notholt, J.; Warneke, T.; Hannigan, J.W.; Warneke, C.; de Gouw, J.A.; Dunlea, E.J.; De Maziere,

M.; Griffith, D.W.T.; Bernath, P.; Jimenez, J.L.; Wennberg, P.O. Importance of secondary sources in the atmospheric budgets of formic and acetic acids. Atmos. Chem. Phys. 2011, 11, 1989-2013.

Pavuluri, C. M.; Kawamura, K.; Swaminathan, T. Water-soluble organic carbon, dicarboxylic acids, ketoacids, and α-dicarbonyls in the tropical Indian aerosols. J. Geophys. Res. 2010, 115, D11302, doi: 10.1029/ 2009JD012661.

Pavuluri, C.M.; Kawamura, K.; Mihalopoulos, N.; Swaminathan, T. Laboratory photochemical processing of aqueous aerosols: formation and degradation of dicarboxylic acids, oxocarboxylic acids and α-dicarbonyls. Atmos. Chem. Phys. 2015, 15, 7999–8012, https://doi.org/10.5194/acp-15-7999-2015.

Pokhrel, A. Studies on ice core records of dicarboxylic acids, ω-oxocarboxylic acids, pyruvic acid, α-dicarbonyls and fatty acids from southern Alaska since 1665 Ad: A link to climate change in the Northern Hemisphere. HUSCAP, 2015, 11786, URI: http://hdl.handle.net/2115/59331.

Pokhrel, A.; Kawamura, K.; Ono, K.; Tsushima, A.; Seki, O.; Matoba, S.; Shiraiwa, T.; Kunwar, B. Ice core records of biomass burning tracers (levoglucosan, dehydroabietic and vanillic acids) from Aurora Peak in Alaska since the 1660s: A new dimension of forest fire activities in the Northern Hemisphere. Atmos. Chem. Phys. Discussion. 2019, doi:10.5194/acp-2019-139.

Pokhrel, A.; Kawamura, K.; Ono, K.; Seki, O.; Fu, P.; Matoba, S.; Shiraiwa, T. Ice core records of monoterpene- and isoprene-SOA tracers from Aurora Peak in Alaska since 1660s: Implication for climate change variability in the North Pacific Rim. Atmos. Environ. 2016, doi: c10.1016/j.atmosenv.2015.09.063.

Pokhrel, A.; Kawamura, K.; Seki, O.; Matoba, S.; Shiraiwa, T. Ice core profiles of saturated fatty acids ($C_{12:0}$ - $C_{30:0}$) and oleic acid ($C_{18:1}$) from southern Alaska since 1734 AD: A link to climate change in the Northern Hemisphere. Atmos. Environ. 2015, 100, 202-209.

Pokhrel, A.; Kawamura, K.; Kunwar, K; Ono, K; Tsushima, A; Seki, O.; Matoba, S.; Shiraiwa, T. Ice core records of levoglucosan and dehydroabietic and vanillic acids from Aurora Peak in Alaska since the 1660s: a proxy signal of biomass-burning activities in the North Pacific Rim. Atmos. Chem. Phys. 2020, 20, 597–612.

Quinn, P.K.; Bates, T.S. The case against climate regulation via oceanic phytoplankton sulphur emissions. Nature. 2011, 480, 51-56, doi:10.1038/nature10580.

Rogge, W. F.; Hildemann, L.M.; Mazurek, M.A.; Cass, G.R.; Simoneit, B.R.T. Sources of fine organic aerosol: Charbroilers and meat cooking operations. Env. Sci. Tech. 1991, 25, 1112-1125.

Rogge, W. F.; Hildemann, L.M.; Mazurek, M.A.; Cass, G.R.; Simoneit, B.R.T. Sources of fine organic aerosol: Pine, oak, and synthetic log combustion in residential fireplaces. Env. Sci. Tech. 1998, 32, 13-22.

Saigne, C., Kirchner, S.; Legrand, M. Ion-chromatographic measurements of ammonium, fluoride, acetate, formate and methanesulphonate ions at very low levels in Antarctic ice. Anal. Chim. 1987, Acta 203, 11–21.

Savarino, J.; Legrand, M. High northern latitude forest fires and vegetation emissions over the last millennium inferred from the chemistry of a central Greenland ice core. J. Geophys. Res. 1998, 103, 8267-8279.

Seinfeld, J.H.; Pandis, S.N. Atmospheric Chemistry and Physics. 1998, John Wiley & Sons, New York.

Sempéré, R.; Kawamura, K. Comparative distributions of dicarboxylic acids and related polar compounds in snow, rain and aerosols from urban atmosphere. Atmos. Environ. 1994, 28, 449-459.

Sempéré, R.; Kawamura, K. Trans-hemispheric contribution of C_2-C_{10} α, ω-dicarboxylic acids and related polar compounds to water soluble organic carbon in the western Pacific aerosols in relation to photochemical oxidation reactions, Global Biogeochemical Cycles. 2003, vol. 17, No. 2, 1069 10.1029/2002GB001980.

Surratt, J.D.; Chan, A.W.H.; Eddingsaasa, N.C.; Chan, M.N.; Loza, C.L.; Kwan, A.J.; Hersey, S.P.; Flagan, R.C.; Wennberg, P.O.; Seinfeld, J.H.; Reactive intermediates revealed in secondary organic aerosol formation from isoprene, PNAS. 2010, 107, 15, 6640-6645.

Surratt, J.D.; Lewandowski, M.; Offenberg, J.H.; Jaoui, M.; Kleindienst, T.E.; Edney, E.O.; Seinfeld, J.H. Effect of acidity on secondary organic aerosol formation from isoprene. Environ. Sci. Technol. 2007, 41, 5363-5369, doi:10.1021/es0704176.

Talbot, R.W.; Mosher, B.W.; Heikes, B.G.; Jacob, D.J.; Munger, J.W.; Daube, B.C.; Keene, W.C.; Maben, J.R.; Artz, R.S. Carboxylic acids in the rural continental atmosphere over the eastern United States during the Shenandoah Cloud and Photochemistry Experiment. J. Geophys. Res. 1995, 100, 9335-9343.

Volkamer, R.; Jimenez, J.L.; Martini, F.S.; Dzepina, K.; Zhang, Q.; Salcedo, D.; Molina, L.T.; Worsnop, D.R.; Molina. M.J. Secondary organic aerosol formation from anthropogenic air pollution: Rapid and higher than expected. Geophys. Res. Lett. 2006, 33, L17811, doi: 10.1029/2006GL026899.

Volkamer, R.; Platt, U.; Wirtz, K. Primary and secondary glyoxal formation from aromatics: Experimental evidence for the bicycloalkyl-radical pathway from benzene, toluene, and p-xylene. J. Phys. Chem. A, 2001, 105, 7865-7874.

Volkamer, R.; Ziemann, P.J.; Molina, M.J. Secondary Organic Aerosol Formation from Acetylene (C2H2): seed effect on SOA yields due to organic photochemistry in the aqueous phase aerosol. Atmos. Chem. Phys. 2009, 9, 1907–1928.

Wang, G.; Kawamura, K.; Lee, S.; Ho, K.; Cao, J. Molecular, seasonal and spatial distribution of organic aerosols from fourteen Chinese cities. Environ. Sci. and Technol. 2006, 40, 4619-4625.

749 Wang, G.; Kawamura, K.; Xie, M.; Hu, S.; Wang, Z. Water-soluble organic compounds in PM2.5 and size-
750 segregated aerosols over Mt. Tai in North China Plain. J. Geophys. Res. 2009, 114, D19208,
751 doi:10.1029/2008JD011390.
752 Wang, K.; Peng, C.; Zhu, Q.; Zhou, X.; Wang, M.; Zhang, K.; Wang, G. Modeling global soil carbon and soil
753 microbial carbon by integrating microbial processes into the ecosystem process model TRIPLEX-GHG.
754 Journal of Advances in Modeling Earth Systems. 2017, 9, 2368–2384,
755 https://doi.org/10.1002/2017MS000920.
756 Wang, S.; Pavuluri, C.M.; Rena, L.; Fu, P.; Zhang, Y.L.; Liu, C-Q. Implications for biomass/coal combustion
757 emissions and secondary formation of carbonaceous aerosols in North China. RSC Adv. 2018, 8, 38108-
758 38117, doi: 10.1039/C8RA06127K.
759 Warneck, P. In-cloud chemistry opens pathway to the formation of oxalic acid in the marine atmosphere. Atmos.
760 Environ. 2003, 37, 2423-2427.
761 Winterhalter, R.; Kippenberger, M.; Williams, J.; Fries, E.; Sieg, K.; Moortgat, G.K. Concentrations of higher
762 dicarboxylic acids C5–C13 in fresh snow samples collected at the High Alpine Research Station Jungfraujoch
763 during CLACE 5 and 6. Atmos. Chem. Phys. 2009, 9, 2097-2112.
764 Zhu, C.; Kawamura, K.; Kunwar, B. Effect of biomass burning over the western North Pacific Rim: wintertime
765 maxima of anhydrosugars in ambient aerosols from Okinawa, Atmos. Chem. Phys. 2015, 15, 1-15. doi:
766 10.5194/acp-15-1-2015.
767

768

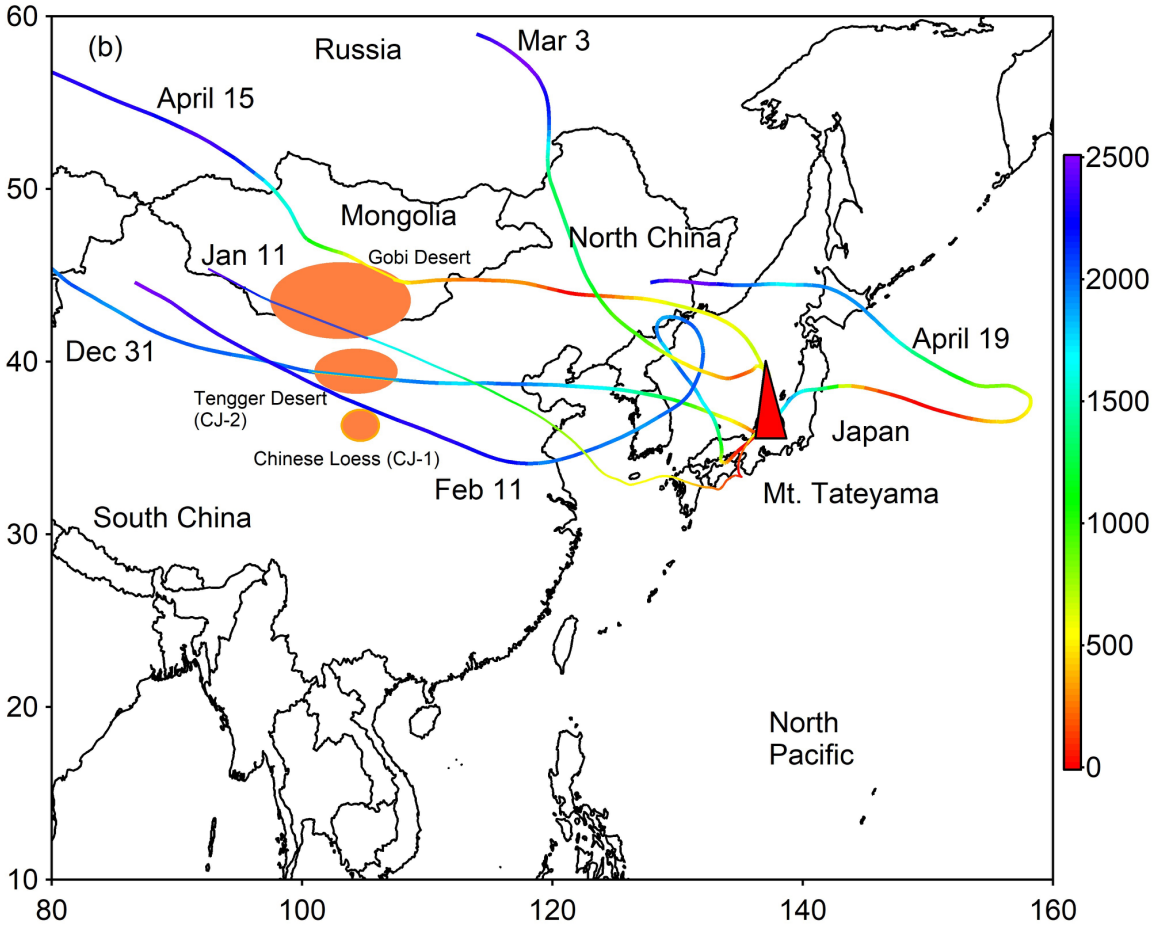

769

770 Figure 1**.** (a) Map showing the geographical region of Murodo-Daira, Mt. Tateyama of Central
771 Japan, 6.5 m long snowpit samples were excavated (19 April, 2008) at elevation of 2450 m
772 a.s.l. and (b) map showing 5 days (2500 m a.s.l. above sea level in meter) backward trajectory
773 analysis of Murodo-Daira, Mt. Tateyama of Central Japan during the snow accumulation
774 period (2007 October to 2008 April).

775

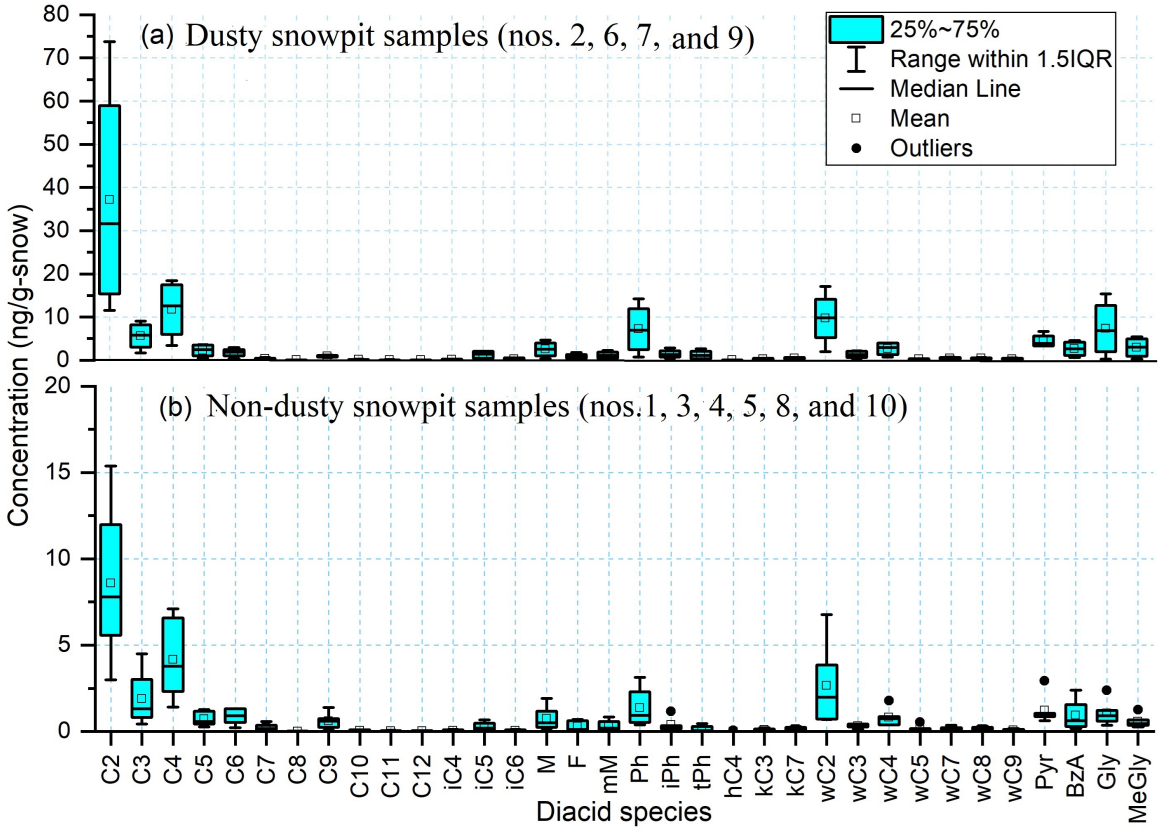

776

777 Figure 2**.** Average molecular distributions of diacids, oxoacids, and α-dicarbonyls in (a) dusty
778 snowpit samples and (b) non-dusty snowpit samples collected from snowpit sequences (6.5 m) at
779 the Murodo-Daira site, Mt. Tateyama in Central Japan.

780

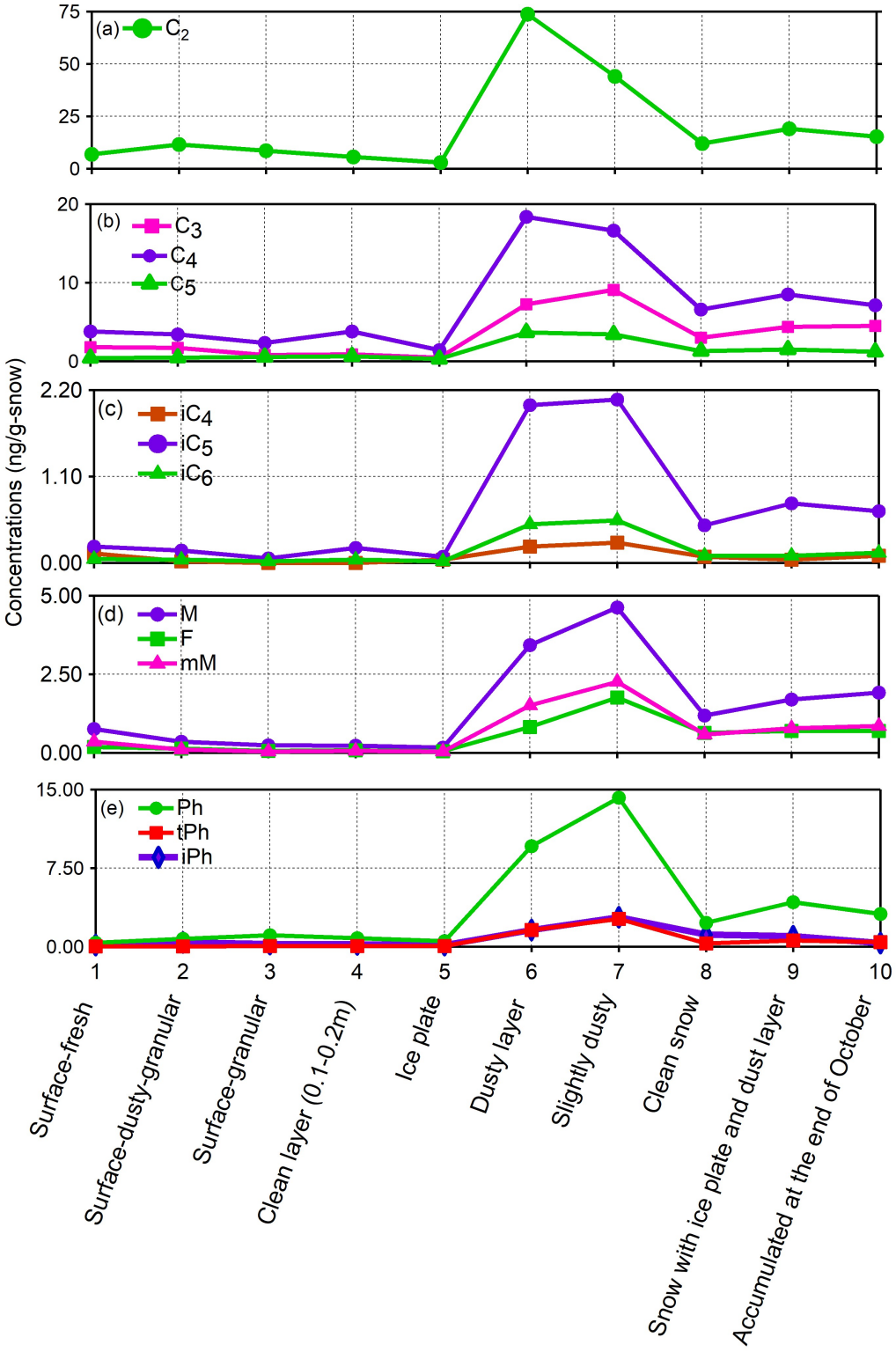

Figure 3. Concentration changes of (a, b) short-chain low molecular weight diacids (s-DCAs) of (a) C_2 (b) C_3, C_4, and C_5, (c) branched-chain saturated diacids (iC_4, iC_5, and iC_6), and (d, e) unsaturated diacids (M, F, mM, Ph, tPh, and iPh) in the snowpit sequences (6.5 m) collected from the Murodo-Daira site, Mt. Tateyama in Central Japan.

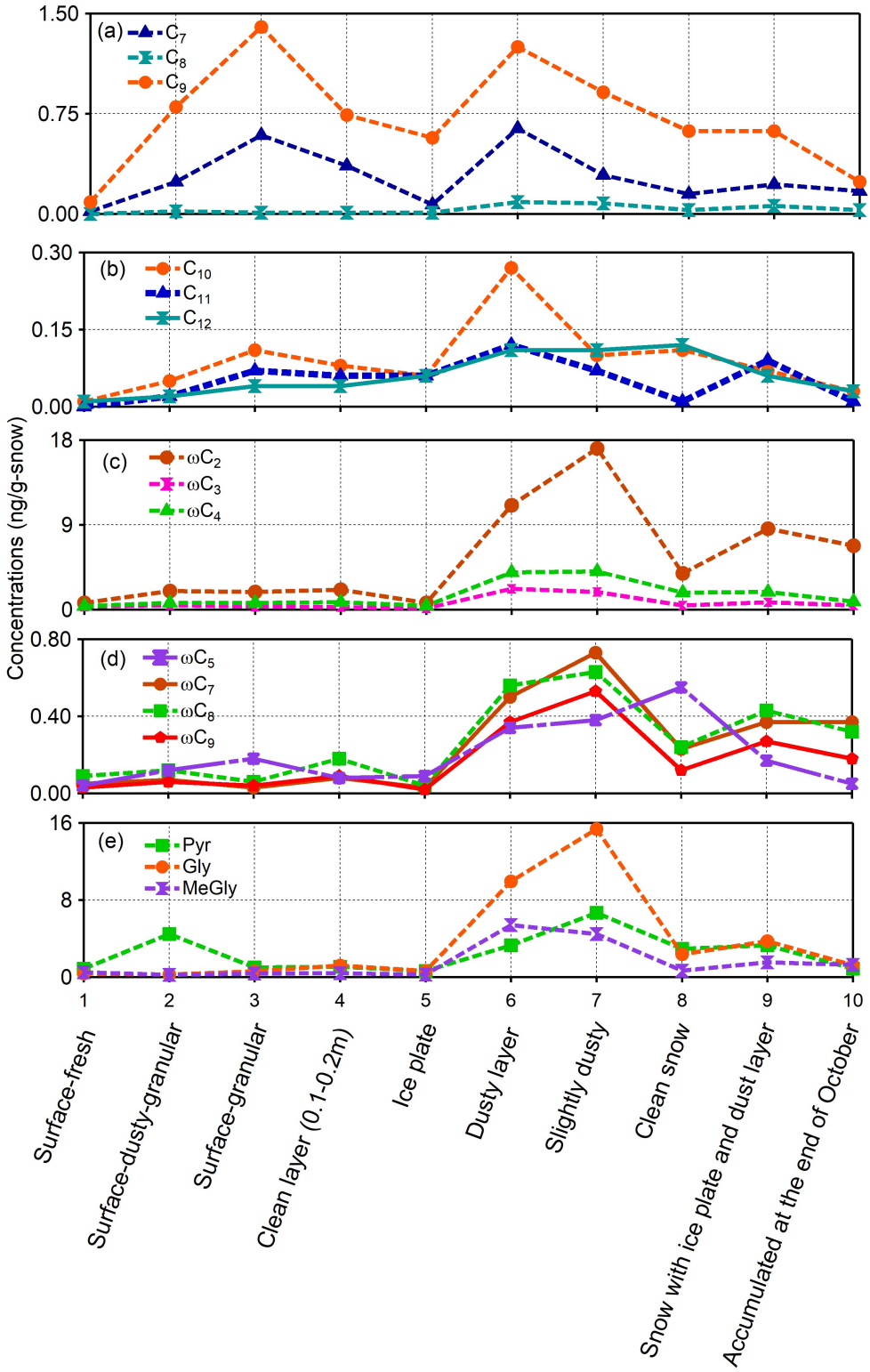

788

789 Figure 4. Concentration changes of long-chain low molecular weight diacids, (a, b) C_7-C_{12},
790 (c, d) oxoacids (ωC_2 - ωC_9), (e) pyruvic acid (Pyr) and α-dicarbonyls (Gly and MeGly) in
791 snowpit sequences (6.5 m) collected from the Murodo-Daira site, Mt. Tateyama in Central
792 Japan.
793

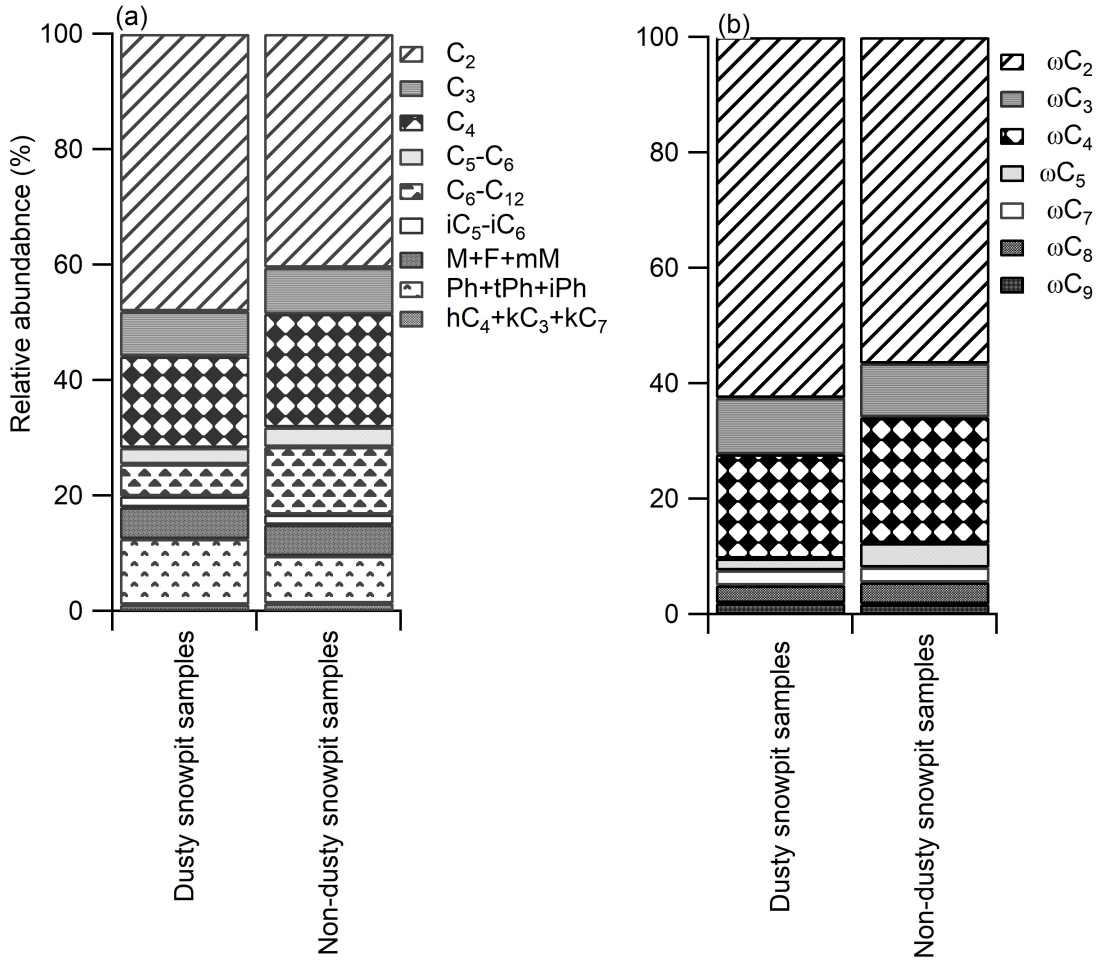

794
795 Figure 5. Relative abundances of (a) diacids and (b) oxoacids in dusty and non-dusty snowpit
796 samples from snowpit sequences (6.5 m) collected from the Murodo-Daira site, Mt. Tateyama
797 in Central Japan.
798

799

Table S1. Descriptions of surface snow samples (Nos. 1-3) collected around a pit site and snowpack samples (Nos. 4-10) collected from a pit (6.6 m in depth) at Murodo-Daira, Mt. Tateyama, Japan (Kawamura et al., 2012).

Sample ID	Depth (m) from the surface	Description
No. 1	Surface	Fresh snow (collected at 10:15 am)
No. 2	Surface	Dusty and granular snow (fresh snow seemed not accumulated due to a strong wind around the site). Dust may be deposited over the snowfield during Asian dust events that were observed on April 14-16, 2008 by lidar over Toyama.
No. 3	Surface	Granular snow (obtained at 15:15 pm). Surface snow melted due to the warmer temperature and stronger radiation in the afternoon and granular snow was collected.
No. 4	0.1-0.2	Clean snow layer
No. 5	0.5	Snow with ice plate (ca. 2 cm thickness). The only ice layer was collected.
No. 6	0.90-1.1	Dusty snow layer. Asian dust event on March 3, 2008 may the source of the dirty layer due to a lidar observation in Toyama.
No. 7	1.2-1.3	Dust layer possibly deposited on February 11, 2008.
No. 8	3.5-3.6	Clean snow layer
No. 9	3.7-3.8	Snow with ice plate and dusts. Dust may have deposited on January 11, 2008.
No. 10	6.4-6.5	Snow accumulated at the end of October 2007

Sampling was conducted from 10:15 to 15:15 on April 19, 2008.
Surface snow samples were collected near the pit site, but the locations were not exactly the same.

800

Table S2. Concentrations of dicarboxylic acids, ω-oxocarboxylic acids, pyruvic acid, and α-dicarbonyls in snow pit samples from the high mountain region of Central Japan in 2008 at Murodo-Daira, Mt. Tateyama.

Concentration (ng/g-snow)		Dust samples (n=4)		Nondust samples (n=6)		Chinese Loess	Tengger dust	Gobi Desert
Compounds	Cn, Abbr.	Min-Max	Ave±Std	Min-Max	Ave±Std	(CJ-1)	(CJ-2)	(G-D)
Oxalic	C_2	12-74	37±28	3-15	8.6±4.5	5090	36672	38589
Malonic	C_3	1.7-9.1	5.6±3.2	0.44-4.5	1.9±1.6	202	1855	1957
Succinic	C_4	3.4-18	12±7	1.4-7.1	4.2±2.3	657	4040	3039
Glutaric	C_5	0.46-3.6	2.3±1.5	0.28-1.3	0.72±0.42	111	660	776
Adipic	C_6	0.34-2.9	1.8±1.1	0.21-1.3	0.78±0.46	70	567	3327
Pimeric	C_7	0.22-0.64	0.35±0.2	0.02-0.59	0.23±0.21	66	714	1160
Suberic	C_8	0.02-0.09	0.06±0.03	0-0.03	0.02±0.01	0	0	1185
Azelaic	C_9	0.62-1.2	0.89±0.26	0.09-1.4	0.61±0.46	182	4557	3888
Sebacic	C_{10}	0.05-0.27	0.12±0.1	0.01-0.11	0.06±0.04	36	2396	2592
Monodecanoic	C_{11}	0.02-0.12	0.08±0.04	0-0.07	0.04±0.03	0	226	6990
Dodecanoic	C_{12}	0.02-0.11	0.08±0.04	0.01-0.06	0.03±0.02	0	0	0
Branched saturated diacids								
Methylmalonic	iC_4	0.02-0.26	0.13±0.12	0-0.12	0.06±0.05	0	0	0
Methylsuccinic	iC_5	0.16-2.08	1.25±0.95	0.06-0.66	0.28±0.24	91	248	144
Methylglutaric	iC_6	0.04-0.54	0.29±0.26	0.02-0.13	0.06±0.04	0	36	0
Unsaturated diacids								
Maleic	C_4, M	0.35-4.6	2.5±1.9	0.17-1.92	0.75±0.7	122	280	597
Fumric	C_4, F	0.14-1.8	0.86±0.67	0.05-0.7	0.29±0.3	352	169	386
Methylmaleic	C_5, mM	0.1-2.26	1.16±0.93	0.04-0.85	0.32±0.34	32	384	267
Phthalic	C_8, Ph	0.75-14	7.2±5.9	0.39-3.1	1.4±1.1	875	4133	1424
Isophthalic	C_8, iPh	0.41-2.8	1.5±1	0.15-1.2	0.38±0.39	0	0	1918
Terephthalic	C_8, tPh	0.03-2.7	1.2±1.2	0.02-0.45	0.16±0.18	0	125	170
Hydroxylated diacids								
Hydroxysuccinic	hC_4	0-0.1	0.05±0.04	0-0.07	0.01±0.03	20	52	45
Ketodiacids								
Ketomalonic	kC_3	0.14-0.46	0.3±0.14	0.01-0.23	0.11±0.09	0	65	174
Ketopimelic	kC_7	0.1-0.62	0.42±0.24	0.06-0.3	0.16±0.1	0	0	40
Total DCAs	0	6.4-328	62±102	5.5-31	17±10	14320	108866	132171
ω-oxocarboxylic acids								
Glyoxylic	ωC_2	1.97-17	9.7±6.3	0.7-6.8	2.7±2.32	347	2061	4412
3-Oxopropanoic	ωC_3	0.48-2.2	1.3±0.84	0.12-0.44	0.32±0.12	36	245	569
4-Oxobutanoic	ωC_4	0.73-4	2.6±1.6	0.39-1.8	0.82±0.51	27	424	543
5-Oxopentanoic	ωC_5	0.12-0.38	0.25±0.13	0.04-0.55	0.17±0.2	35	60	243
7-oxoheptanoic	ωC_7	0.07-0.73	0.42±0.27	0.03-0.37	0.13±0.14	21	345	337
8-Oxoctanoic	ωC_8	0.12-0.63	0.43±0.23	0.04-0.32	0.16±0.11	0	58	110
9-Oxononoic	ωC_9	0.06-0.53	0.31±0.2	0.02-0.18	0.08±0.06	22	34	853
Total w-oxoacids		1.4-26	8.6±8.3	1.3-10	4.4±3.4			
Pyruvic	C3, Pyr	0.63-6.7	2.51±2	0.63-2.9	1.2±0.85	178	975	1549
α-dicarbonyls								
Glyoxal	C_2, Gly	0.27-15	3.6±5.1	0.37-2.4	1.1±0.73	81	546	667
Methylglyoxal	C_3, MeGly	0.22-5.4	1.5±1.9	0.27-1.3	0.58±0.36	45	300	541
Total a-dicarbonyls	0	0.49-20.4	10.2±9.1	0.64-3.7	1.68±1.09	126	846	1208

806 **Figure S1:** Correlation plots of oxalic acid with (a) glyoxylic acid (ωC_2), (b) glyoxal (Gly), (c)
807 methylglyoxal (MeGly), and (d) pyruvic acid (Pyr) in snowpit samples collected from the
808 Murodo-Daira site, Mt. Tateyama in Central Japan. Red open circle and green closed square
809 indicate non-dusty and dusty snowpit (excluding no.6) samples, respectively.
810

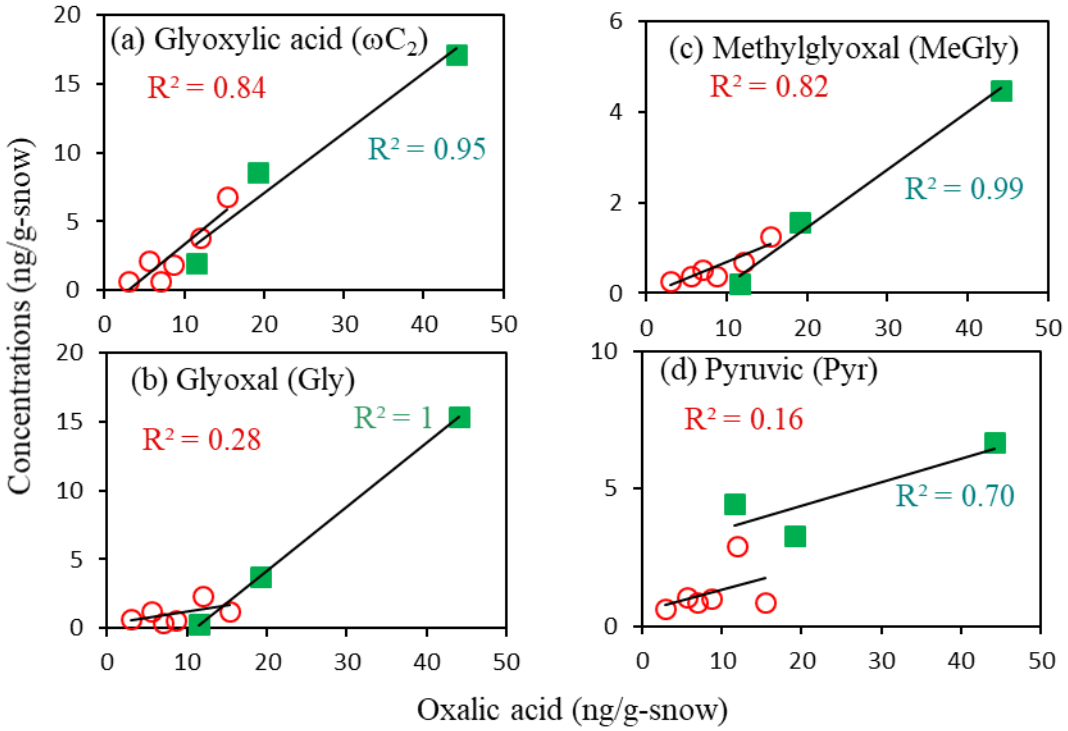

811
812

Figure S2: Correlation plots (red and green colors indicate the non dusty and dusty samples, respectively) of suberic acid with (a) oxalic (C_2), (b) malonic (C_3), (c) succinic (C_4) (d) glutaric (C_5), (e) undecanedioic acid (C_{11}: sample no. 1 has zero concentration), and (f) azelaic acid (C_9) in snowpit samples (excluding no.6) collected from the Murodo-Daira site, Mt. Tateyama in Central Japan.

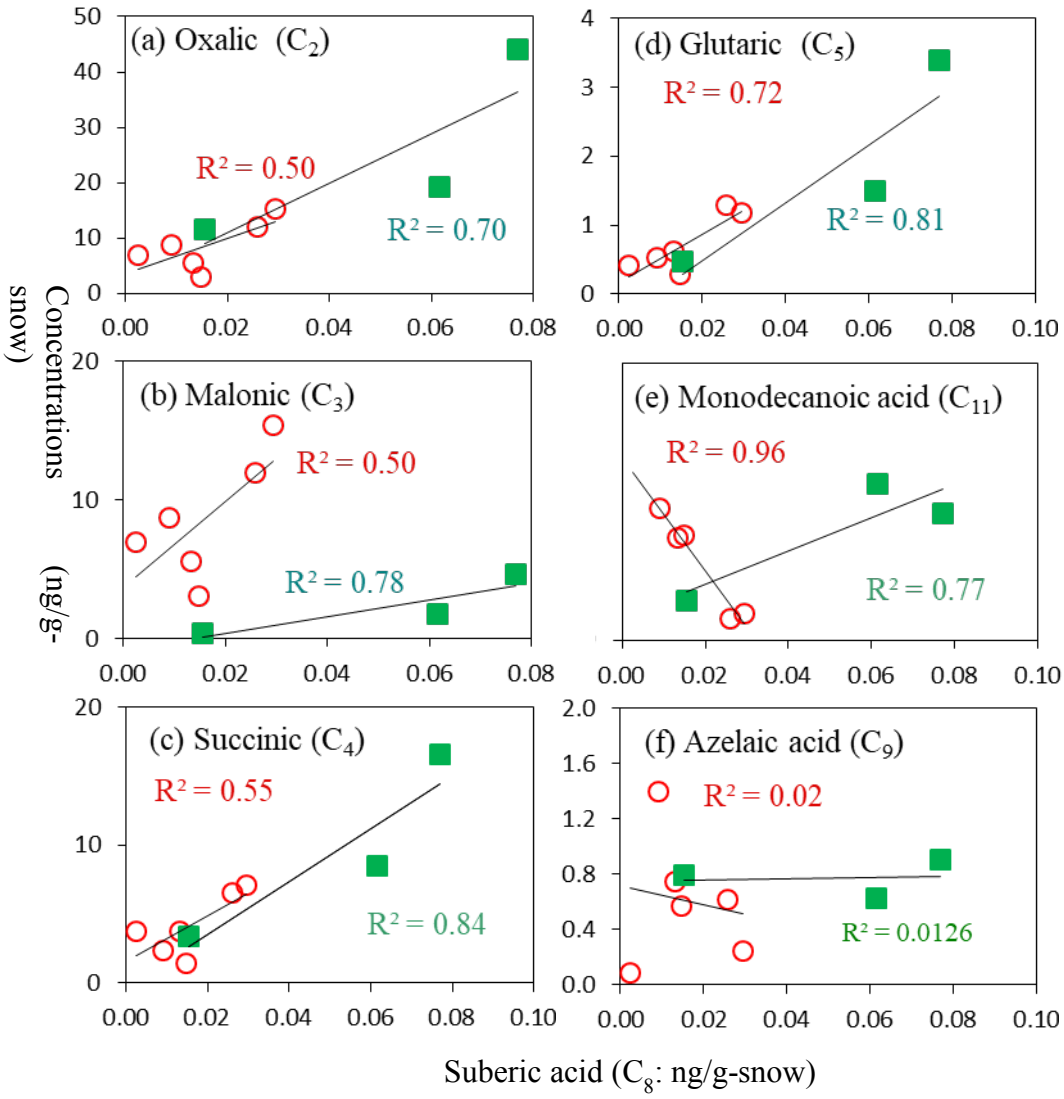

820 **Figure S3**. Correlation plots of phthalic and benzoic acids (red and green colors indicate the non dusty and dusty
821 samples, respectively) with (a) methylmaleic (mM), (b) fumaric (F), (c) maleic (M), (d) glyoxal (Gly), (e)
822 methylglyoxal, and (f) oxalic acid with phthalic acid, and (g) methylmaleic (mM), (h) fumaric (F), (i) maleic (M),
823 (j) glyoxal (Gly), (k) methylglyoxal, and (l) oxalic acid in snowpit samples (excluding no.6) collected from the
824 Murodo-Daira site, Mt. Tateyama in Central Japan.